

## Fine-Tuning of Copper(I)-Dioxygen Reactivity by 2-(2-Pyridyl)ethylamine Bidentate Ligands

Masayasu Taki,<sup>‡</sup> Shinichi Teramae,<sup>‡</sup> Shigenori Nagatomo,<sup>§</sup> Yoshimitsu Tachi,<sup>†</sup>  
Teizo Kitagawa,<sup>§</sup> Shinobu Itoh,<sup>\*,†</sup> and Shunichi Fukuzumi<sup>\*,‡</sup>

Contribution from the Department of Chemistry, Graduate School of Science, Osaka City University, 3-3-138 Sugimoto, Sumiyoshi-ku, Osaka 558-8585, Japan, Department of Material and Life Science, Graduate School of Engineering, Osaka University, CREST, Japan Science and Technology Corporation, 2-1 Yamada-oka, Suita, Osaka 565-0871, Japan, and Institute for Molecular Science, Myodaiji, Okazaki 444-8585, Japan

Received January 27, 2002

**Abstract:** Copper(I)-dioxygen reactivity has been examined using a series of 2-(2-pyridyl)ethylamine bidentate ligands  $R^1Py1^{R2,R3}$ . The bidentate ligand with the methyl substituent on the pyridine nucleus  $MePy1^{Et,Bz}$  (*N*-benzyl-*N*-ethyl-2-(6-methylpyridin-2-yl)ethylamine) predominantly provided a ( $\mu$ - $\eta^2$ : $\eta^2$ -peroxo)-dicopper(II) complex, while the bidentate ligand without the 6-methyl group  $^HPy1^{Et,Bz}$  (*N*-benzyl-*N*-ethyl-2-(2-pyridyl)ethylamine) afforded a bis( $\mu$ -oxo)dicopper(III) complex under the same experimental conditions. Both  $Cu_2O_2$  complexes gradually decompose, leading to oxidative *N*-dealkylation reaction of the benzyl group. Detailed kinetic analysis has revealed that the bis( $\mu$ -oxo)dicopper(III) complex is the common reactive intermediate in both cases and that O–O bond homolysis of the peroxo complex is the rate-determining step in the former case with  $MePy1^{Et,Bz}$ . On the other hand, the copper(I) complex supported by the bidentate ligand with the smallest *N*-alkyl group ( $^HPy1^{Me,Me}$ , *N,N*-dimethyl-2-(2-pyridyl)ethylamine) reacts with molecular oxygen in a 3:1 ratio in acetone at a low temperature to give a mixed-valence trinuclear copper(II, II, III) complex with two  $\mu_3$ -oxo bridges, the UV–vis spectrum of which is very close to that of an active oxygen intermediate of lacase. Detailed spectroscopic analysis on the oxygenation reaction at different concentrations has indicated that a bis( $\mu$ -oxo)dicopper(III) complex is the precursor for the formation of trinuclear copper complex. In the reaction with 2,4-di-*tert*-butylphenol (DBP), the trinuclear copper(II, II, III) complex acts as a two-electron oxidant to produce an equimolar amount of the C–C coupling dimer of DBP (3,5,3',5'-tetra-*tert*-butyl-biphenyl-2,2'-diol) and a bis( $\mu$ -hydroxo)dicopper(II) complex. Kinetic analysis has shown that the reaction consists of two distinct steps, where the first step involves a binding of DBP to the trinuclear complex to give a certain intermediate that further reacts with the second molecule of DBP to give another intermediate, from which the final products are released. Steric and/or electronic effects of the 6-methyl group and the *N*-alkyl substituents of the bidentate ligands on the copper(I)-dioxygen reactivity have been discussed.

### Introduction

A growing amount of information about copper(I)-dioxygen reactivity has recently been accumulated, providing profound insight into the mechanism of  $O_2$ -binding and activation at copper reaction sites involved in many biological systems as well as in a variety of catalytic oxidation processes.<sup>1–7</sup> The most

thoroughly investigated is the dinuclear copper-dioxygen species  $Cu_2O_2$ , where 2-(2-pyridyl)ethylamine derivatives have played important roles as the supporting ligands. The dinucleating ligand (XYL) containing two bis[2-(2-pyridyl)ethyl]amine *tridentate* metal binding units connected by *m*-xylyl group (Chart 1) was first reported by Karlin and co-workers to develop a functional model of tyrosinase, in which aromatic moiety of the *m*-xylyl group was quantitatively hydroxylated in the reaction of its dinuclear copper(I) complex and dioxygen.<sup>8</sup> Reversible dioxygen binding (functional model of hemocyanin) was also accomplished by the same research group using a series of dinucleating ligands which consist of the same *tridentate*

\* To whom correspondence should be addressed. E-mail: shinobu@sci.osaka-cu.ac.jp, fukuzumi@chem.eng.osaka-u.ac.jp.

<sup>†</sup> Osaka City University.

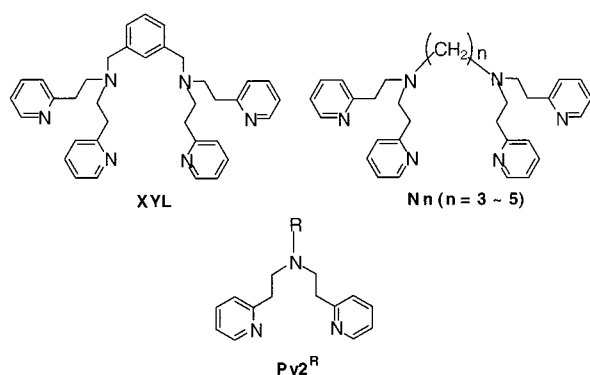
<sup>‡</sup> Osaka University.

<sup>§</sup> Institute for Molecular Science.

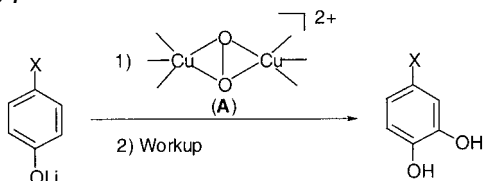
- (1) Karlin, K. D.; Tyeklár, Z., Eds. *Inorganic Chemistry of Copper*; Chapman & Hall: New York, 1993.
- (2) Fox, S.; Karlin, K. D. In *Active Oxygen in Biochemistry*; Valentine, J. S., Foote, C. S., Greenberg, A., Liebman, J. F., Eds.; Chapman and Hall: London, 1995; pp 188–231.
- (3) Ito, M.; Fujisawa, K.; Kitajima, N.; Moro-oka, Y. In *Oxygenases and Model Systems*; Funabiki, T., Ed.; Kluwer Academic Publishers: Dordrecht, 1997; pp 345–376.
- (4) Blackman, A. G.; Tolman, W. B. In *Metal-Oxo and Metal-Peroxo Species in Catalytic Oxidations*; Meunier, B., Ed.; Springer: Berlin, 2000; pp 179–211.

- (5) Kopf, M.-A.; Karlin, K. D. In *Biomimetic Oxidations Catalyzed by Transition Metal Complexes*; Meunier, B., Ed.; Imperial College Press: London, 1999; pp 309–362.
- (6) Solomon, E. I.; Sundaram, U. M.; Machonkin, T. E. *Chem. Rev.* **1996**, *96*, 2563–2605.
- (7) Klinman, J. P. *Chem. Rev.* **1996**, *96*, 2541–2561.
- (8) Karlin, K. D.; Gultneh, Y.; Hutchinson, J. P.; Zubieta, J. *J. Am. Chem. Soc.* **1982**, *104*, 5240–5242.

Chart 1



Scheme 1



metal binding units connected by C<sub>3</sub>–C<sub>5</sub> alkyl linker chains (Chart 1, Nn;  $n = 3-5$ ).<sup>9</sup> In these reactions, ( $\mu$ - $\eta^2$ : $\eta^2$ -peroxy)-dicopper(II) species have been identified as the Cu<sub>2</sub>O<sub>2</sub> intermediate, for which they assigned a bent structure (butterfly shape) due to the structural restriction induced by the alkyl linker groups.<sup>10,11</sup> The side-on peroxy dicopper(II) complexes having a flat structure can also be assessed by the oxygenation reaction of mononuclear copper(I) complexes supported by a series of *N*-alkyl-bis[2-(2-pyridyl)ethyl]amine tridentate ligands (Py2<sup>R</sup> in Chart 1).<sup>12-15</sup> The ( $\mu$ - $\eta^2$ : $\eta^2$ -peroxy)dicopper(II) complex (A) thus formed has recently been demonstrated to have an ability to hydroxylate phenolates to the corresponding catechols via an electrophilic aromatic substitution mechanism, providing important mechanistic insight into the phenolase activity of tyrosinase (Scheme 1).<sup>15</sup>

Another important finding of this series is the aliphatic ligand hydroxylation in the reaction of copper(I) complex of Py2<sup>Phe</sup> [R = -CH<sub>2</sub>CH<sub>2</sub>Ph (Phe) in Chart 1] and O<sub>2</sub>.<sup>16,17</sup> In this case as well, a ( $\mu$ - $\eta^2$ : $\eta^2$ -peroxy)dicopper(II) complex (A) has been identified as an initially formed intermediate.<sup>13</sup> However, detailed kinetic analysis on this reaction has suggested that the ( $\mu$ - $\eta^2$ : $\eta^2$ -peroxy)dicopper(II) complex (A) is not the real active species, but, instead, another type of Cu<sub>2</sub>O<sub>2</sub>-intermediate derived from the peroxy complex (A) is involved as the real active

Scheme 2

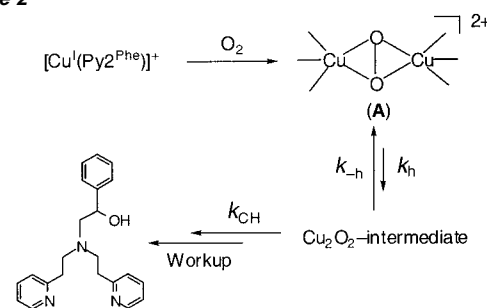
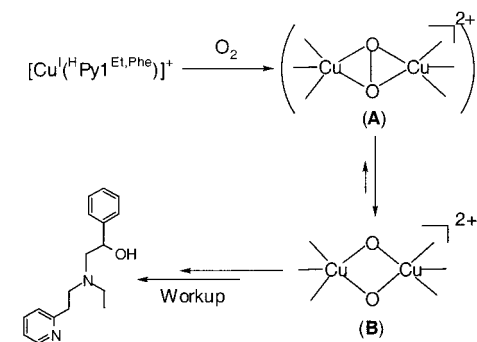


Chart 2

R <sup>1</sup>	R <sup>2</sup>	R <sup>3</sup>	R <sup>1</sup> Py <sup>1</sup> R <sup>2</sup> ,R <sup>3</sup>
H	-C <sub>2</sub> H <sub>5</sub>	-CH <sub>2</sub> Ph	<sup>H</sup> Py <sub>1</sub> <sup>Et,Bz</sup>
H	-C <sub>2</sub> H <sub>5</sub>	-CD <sub>2</sub> Ph	<sup>H</sup> Py <sub>1</sub> <sup>Et,Bz-d2</sup>
Me	-C <sub>2</sub> H <sub>5</sub>	-CH <sub>2</sub> Ph	<sup>Me</sup> Py <sub>1</sub> <sup>Et,Bz</sup>
Me	-C <sub>2</sub> H <sub>5</sub>	-CD <sub>2</sub> Ph	<sup>Me</sup> Py <sub>1</sub> <sup>Et,Bz-d2</sup>
H	-C <sub>2</sub> H <sub>5</sub>	-C <sub>2</sub> H <sub>4</sub> Ph	<sup>H</sup> Py <sub>1</sub> <sup>Et,Phe</sup>
H	-C <sub>2</sub> H <sub>5</sub>	-C <sub>2</sub> D <sub>4</sub> Ph	<sup>H</sup> Py <sub>1</sub> <sup>Et,Phe-d4</sup>
H	-CH <sub>3</sub>	-CH <sub>3</sub>	<sup>H</sup> Py <sub>1</sub> <sup>Me,Me</sup>

Scheme 3



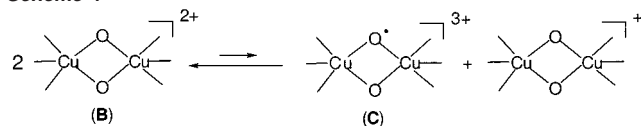
intermediate (Scheme 2).<sup>13</sup> Ligand modification from the tridentate (Py2<sup>Phe</sup>) to bidentate (<sup>H</sup>Py1<sup>Et,Phe</sup>, Chart 2) resulted in formation of a bis( $\mu$ -oxo)dicopper(III) intermediate (B), from which the same type of aliphatic ligand hydroxylation occurred at its benzylic position of the phenethyl sidearm (Scheme 3).<sup>18</sup> Thus, we concluded that the bis( $\mu$ -oxo)dicopper(III) complex (B) was the real active oxygen intermediate both in the Py2<sup>Phe</sup> and in the <sup>H</sup>Py1<sup>Et,Phe</sup> ligand systems and that the bidentate ligand enhanced the O–O bond homolysis of the ( $\mu$ - $\eta^2$ : $\eta^2$ -peroxy)-dicopper(II) (A) to give the bis( $\mu$ -oxo)dicopper(III) complex (B) predominantly.<sup>18</sup> Detailed kinetic studies have also indicated that the aliphatic ligand hydroxylation proceeds via hydrogen atom abstraction by the high valent copper-oxo species in B and subsequent oxygen rebound mechanism or its concerted variant.<sup>18</sup> The bis( $\mu$ -oxo)dicopper(III) complex supported by the bidentate ligand <sup>H</sup>Py1<sup>Et,Bz-d2</sup> (Chart 2) has recently been shown to have an ability to oxo-transfer reaction toward sulfides.<sup>19</sup> Furthermore, it has been demonstrated that a disproportionation reaction of B could occur to afford a more reactive intermediate such as a ( $\mu$ -oxo)( $\mu$ -oxyl radical)dicopper(III) species (C) (Scheme 4). Such an oxyl radical dicopper(III) species can

- (9) Karlin, K. D.; Haka, M. S.; Cruse, R. W.; Gultneh, Y. *J. Am. Chem. Soc.* **1985**, *107*, 5828–5829.
- (10) Pidcock, E.; Obias, H. V.; Zhang, C. X.; Karlin, K. D.; Solomon, E. I. *J. Am. Chem. Soc.* **1998**, *120*, 7841–7847.
- (11) Pidcock, E.; Obias, H. V.; Abe, M.; Liang, H.-C.; Karlin, K. D.; Solomon, E. I. *J. Am. Chem. Soc.* **1999**, *121*, 1299–1308.
- (12) Sanyal, I.; Mahroof-Tahir, M.; Nasir, M. S.; Ghosh, P.; Cohen, B. I.; Gultneh, Y.; Cruse, R. W.; Farooq, A.; Karlin, K. D.; Liu, S.; Zubieta, J. *Inorg. Chem.* **1992**, *31*, 4322–4332.
- (13) Itoh, S.; Nakao, H.; Berreau, L. M.; Kondo, T.; Komatsu, M.; Fukuzumi, S. *J. Am. Chem. Soc.* **1998**, *120*, 2890–2899.
- (14) Pidcock, E.; DeBeer, S.; Obias, H. V.; Hedman, B.; Hodgson, K. O.; Karlin, K. D.; Solomon, E. I. *J. Am. Chem. Soc.* **1999**, *121*, 1870–1878.
- (15) Itoh, S.; Kumei, H.; Taki, M.; Nagatomo, S.; Kitagawa, T.; Fukuzumi, S. *J. Am. Chem. Soc.* **2001**, *123*, 6708–6709.
- (16) Itoh, S.; Kondo, T.; Komatsu, M.; Ohshiro, Y.; Li, C.; Kanehisa, N.; Kai, Y.; Fukuzumi, S. *J. Am. Chem. Soc.* **1995**, *117*, 4714–4715.
- (17) Réglér et al. reported closely related systems: (a) Blain, I.; Bruno, P.; Giorgi, M.; Lojou, E.; Lexa, D.; Réglér, M. *Eur. J. Inorg. Chem.* **1998**, 1297–1304. (b) Blain, I.; Giorgi, M.; De Raggi, I.; Réglér, M. *Eur. J. Inorg. Chem.* **2000**, 393–398. (c) Blain, I.; Giorgi, M.; De Raggi, I.; Réglér, M. *Eur. J. Inorg. Chem.* **2001**, 205–211.

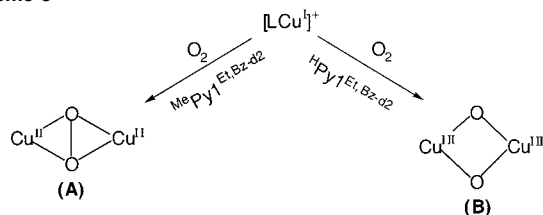
- (18) Itoh, S.; Taki, M.; Nakao, H.; Holland, P. L.; Tolman, W. B.; Que, L., Jr.; Fukuzumi, S. *Angew. Chem.* **2000**, *112*, 409–411; *Angew. Chem., Int. Ed.* **2000**, *39*, 398–400.

- (19) Taki, M.; Itoh, S.; Fukuzumi, S. *J. Am. Chem. Soc.* **2002**, *124*, 998–1002.

## Scheme 4



## Scheme 5



participate in the C–H bond activation of external substrates such as 1,4-cyclohexadiene and related substrates.<sup>20</sup> Thus, the reactivity studies of the Cu<sub>2</sub>O<sub>2</sub> complexes using the *tridentate* and *bidentate* ligands have provided significantly important information about the dioxygen activation mechanism at the dinuclear copper reaction centers. However, fine-tuning of copper(I)-dioxygen reactivity by the subtle ligand modification of bidentate or tridentate ligands has yet to be achieved.

We report herein that a small perturbation of the ligand structure of the bidentate ligands (Chart 2) leads to drastic changes in the structure and reactivity of the reactive Cu<sub>2</sub>O<sub>2</sub> intermediates. The side-on peroxo dicopper(II) complex (A) and the bis( $\mu$ -oxo)dicopper(III) complex (B) as well as a mixed-valence trinuclear copper(II, II, III) complex with two  $\mu_3$ -oxo bridges exhibiting a similar absorption spectrum of an active oxygen intermediate of laccase (E, see Scheme 6)<sup>21</sup> have been assessed by using the simple *bidentate ligands* MePy1<sup>Et,Bz</sup>, HPy1<sup>Et,Bz</sup>, and HPy1<sup>Me,Me</sup>, respectively (Chart 2). The reactivity of such dinuclear and trinuclear copper-dioxygen complexes and the formation mechanism have been investigated in detail to provide profound insight into the mechanism of dioxygen activation and multielectron reduction of dioxygen to water at dinuclear and trinuclear copper reaction centers in biological systems.

## Results and Discussion

**Synthesis and Characterization of Ligands and Copper(I) Complexes.** The bidentate ligands HPy1<sup>Et,Bz</sup> and MePy1<sup>Et,Bz</sup> (Chart 2) were prepared by Michael addition of benzylamine to 2-vinylpyridine or 6-methyl-2-vinylpyridine in refluxing methanol in the presence of an equimolar amount of acetic acid. The resulting monoalkylated 2-(2-pyridyl)ethylamine derivatives were then treated with ethyl bromide in refluxing methanol to give HPy1<sup>Et,Bz</sup> and MePy1<sup>Et,Bz</sup>, respectively. The diderated ligands at their benzylic position, HPy1<sup>Et,Bz-d2</sup> and MePy1<sup>Et,Bz-d2</sup>, were prepared in the same way using PhCD<sub>2</sub>NH<sub>2</sub> instead of PhCH<sub>2</sub>NH<sub>2</sub>. Ligand HPy1<sup>Me,Me</sup> was prepared by reductive alkylation of 2-(2-pyridyl)ethylamine using paraformaldehyde and NaBH<sub>3</sub>CN in MeOH–water (9:1) containing acetic acid at room temperature.

Treatment of the bidentate ligands HPy1<sup>Et,Bz(-d2)</sup> and MePy1<sup>Et,Bz(-d2)</sup> with an equimolar amount of [Cu<sup>I</sup>(CH<sub>3</sub>CN)<sub>4</sub>]<sup>+</sup>PF<sub>6</sub><sup>-</sup>

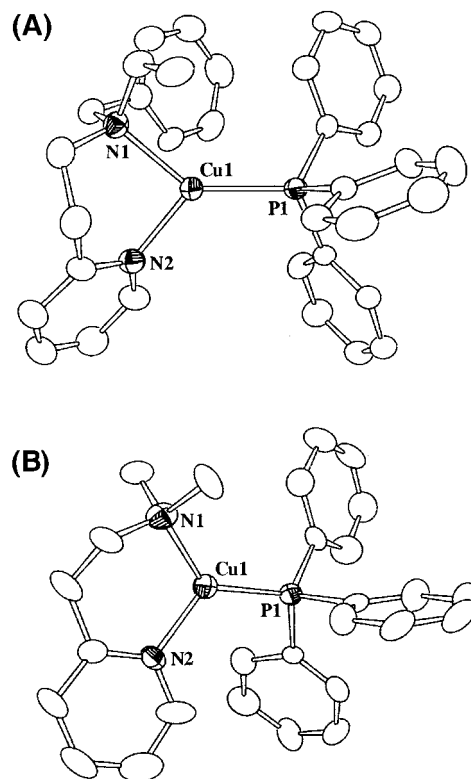


**Figure 1.** ORTEP drawings of the cationic parts of [Cu(HPy1<sup>Et,Bz-d2</sup>)(PPh<sub>3</sub>)]PF<sub>6</sub> (A) and [Cu(HPy1<sup>Me,Me</sup>)(PPh<sub>3</sub>)]PF<sub>6</sub> (B) showing 50% probability thermal-ellipsoid. Hydrogen atoms and counteranions are omitted for clarity.

in THF under anaerobic conditions (in a glovebox) gave the corresponding copper(I) complexes, in which one CH<sub>3</sub>CN molecule is involved as an external ligand to complete a three-coordinate trigonal planar structure (see Experimental Section). Reaction of HPy1<sup>Me,Me</sup> with an equimolar amount of [Cu<sup>I</sup>(CH<sub>3</sub>CN)<sub>4</sub>]<sup>+</sup>CF<sub>3</sub>SO<sub>3</sub><sup>-</sup> in acetone also gave the corresponding copper(I) complex under anaerobic conditions. In this case, CF<sub>3</sub>SO<sub>3</sub><sup>-</sup> binds to the metal center, but no acetonitrile molecule is involved. Such a three-coordinate copper(I) complex with a trigonal planar structure has been structurally characterized by using air-stable phosphine complexes. Thus, the treatment of the copper(I) complexes with PPh<sub>3</sub> gave the copper(I)-phosphine complexes, [Cu<sup>I</sup>(HPy1<sup>Et,Bz-d2</sup>)(PPh<sub>3</sub>)]PF<sub>6</sub> and [Cu<sup>I</sup>(HPy1<sup>Me,Me</sup>)(PPh<sub>3</sub>)]PF<sub>6</sub>, for which X-ray crystallographic analyses have been performed as shown in Figure 1. The crystallographic data and selected bond lengths and angles of them are summarized in Tables 1 and 2, respectively.

The copper(I)-phosphine complex [Cu<sup>I</sup>(HPy1<sup>Et,Bz-d2</sup>)(PPh<sub>3</sub>)]PF<sub>6</sub> exhibits a trigonal planar structure in which the copper ion exists just on the N(1)–N(2)–P(1) plane (Figure 1A). [Cu<sup>I</sup>(HPy1<sup>Me,Me</sup>)(PPh<sub>3</sub>)]PF<sub>6</sub> (Figure 1B) also exhibits a trigonal planar structure with little deviation (0.14 Å) of the copper ion from the N(1)–N(2)–P(1) plane. In the case of [Cu<sup>I</sup>(HPy1<sup>Et,Bz-d2</sup>)(PPh<sub>3</sub>)]PF<sub>6</sub>, the Cu(1)–N(1) and Cu(1)–N(2) bonds are slightly elongated as compared to those values of [Cu<sup>I</sup>(HPy1<sup>Me,Me</sup>)(PPh<sub>3</sub>)]PF<sub>6</sub> ( $\Delta d_{\text{Cu}(1)-\text{N}(1)} = 0.07 \text{ \AA}$ ,  $\Delta d_{\text{Cu}(1)-\text{N}(2)} = 0.032 \text{ \AA}$ ), and the angle of N(1)–Cu(1)–N(2) becomes smaller (93.9° for [Cu<sup>I</sup>(HPy1<sup>Et,Bz-d2</sup>)(PPh<sub>3</sub>)]PF<sub>6</sub> and 102.2° for [Cu<sup>I</sup>(HPy1<sup>Me,Me</sup>)(PPh<sub>3</sub>)]PF<sub>6</sub>, see Table 2). These structural differences between the two copper(I) complexes could be attributed to a steric repulsion between the bulkier *N*-alkyl groups and the copper(I) ion in the HPy1<sup>Et,Bz-d2</sup> system. Such steric effects of the *N*-alkyl

(20) Taki, M.; Itoh, S.; Fukuzumi, S. *J. Am. Chem. Soc.* **2001**, *123*, 6203–6204.

(21) Cole, A. P.; Root, D. E.; Mukherjee, P.; Solomon, E. I.; Stack, T. D. P. *Science* **1996**, *273*, 1848–1850.

**Table 1.** Summary of X-ray Crystallographic Data

	[Cu <sup>I</sup> ( <sup>H</sup> Py <sup>1</sup> <sup>Et,Bz-d2</sup> )(PPh <sub>3</sub> )]PF <sub>6</sub> ·H <sub>2</sub> O	[Cu <sup>I</sup> ( <sup>H</sup> Py <sup>1</sup> <sup>Me,Me</sup> )(PPh <sub>3</sub> )]PF <sub>6</sub>	[Cu <sup>II</sup> <sub>2</sub> ( <sup>H</sup> Py <sup>1</sup> <sup>Me,Me</sup> ) <sub>2</sub> (μ-OH) <sub>2</sub> ](CF <sub>3</sub> SO <sub>3</sub> ) <sub>2</sub>
empirical formula	C <sub>34</sub> H <sub>35</sub> D <sub>2</sub> N <sub>2</sub> O <sub>2</sub> P <sub>2</sub> F <sub>6</sub> Cu	C <sub>27</sub> H <sub>29</sub> N <sub>2</sub> P <sub>2</sub> F <sub>6</sub> Cu	C <sub>20</sub> H <sub>30</sub> N <sub>4</sub> O <sub>8</sub> S <sub>2</sub> F <sub>6</sub> Cu <sub>2</sub>
formula weight	731.15	621.02	759.68
crystal system	monoclinic	orthorhombic	monoclinic
space group	<i>P2<sub>1</sub>/n</i> (No. 14)	<i>Pna2<sub>1</sub></i> (No. 33)	<i>P2<sub>1</sub>/c</i> (No. 14)
<i>a</i> , Å	14.3075(3)	22.512(2)	10.515(1)
<i>b</i> , Å	14.7516(4)	8.2258(7)	12.2207(8)
<i>c</i> , Å	16.6486(4)	14.925(1)	12.041(1)
β, deg	103.4220(7)		106.414(3)
<i>V</i> , Å <sup>3</sup>	3417.9(1)	2763.7(4)	1484.2(2)
<i>Z</i>	4	4	2
<i>D</i> <sub>calc</sub> , g/cm <sup>3</sup>	1.466	1.492	1.700
<i>T</i> , °C	−115	−50	23
crystal size, mm	0.20 × 0.20 × 0.10	0.20 × 0.20 × 0.10	0.40 × 0.40 × 0.50
μ (Mo Kα), cm <sup>−1</sup>	7.98	9.66	16.60
no. of reflns measd	31 595	22 498	3546
no. of reflns obsd	5056 [ <i>I</i> > 1.0σ( <i>I</i> )]	3053 [ <i>I</i> > 0.8σ( <i>I</i> )]	2442 [ <i>I</i> > 0.8σ( <i>I</i> )]
no. of variables	441	344	206
<i>R</i> <sup>a</sup>	0.057	0.043	0.045
<i>R</i> <sub>w</sub> <sup>b</sup>	0.087	0.034	0.079

$$^a R = \sum ||F_o| - |F_c|| / \sum |F_o|. \quad ^b R_w = \{ \sum w(|F_o| - |F_c|)^2 / \sum w F_o^2 \}^{1/2}.$$

**Table 2.** Selected Bond Lengths (Å) and Angles (deg)

	[Cu <sup>I</sup> ( <sup>H</sup> Py <sup>1</sup> <sup>Et,Bz-d2</sup> )(PPh <sub>3</sub> )]PF <sub>6</sub>		
Cu(1)–N(1)	2.108(4)	N(1)–Cu(1)–N(2)	93.80(18)
Cu(1)–N(2)	2.020(5)	N(1)–Cu(1)–P(1)	137.99(13)
Cu(1)–P(1)	2.1821(14)	N(2)–Cu(1)–P(1)	128.03(14)
	[Cu <sup>I</sup> ( <sup>H</sup> Py <sup>1</sup> <sup>Me,Me</sup> )(PPh <sub>3</sub> )]PF <sub>6</sub>		
Cu(1)–N(1)	2.082(7)	N(1)–Cu(1)–N(2)	102.5(3)
Cu(1)–N(2)	1.989(6)	N(1)–Cu(1)–P(1)	133.2(2)
Cu(1)–P(1)	2.176(2)	N(2)–Cu(1)–P(1)	122.7(2)
	[Cu <sup>II</sup> <sub>2</sub> ( <sup>H</sup> Py <sup>1</sup> <sup>Me,Me</sup> ) <sub>2</sub> (μ-OH) <sub>2</sub> ](CF <sub>3</sub> SO <sub>3</sub> ) <sub>2</sub>		
Cu(1)–N(1)	2.066(3)	N(1)–Cu(1)–N(2)	95.07(11)
Cu(1)–N(2)	2.001(3)	N(1)–Cu(1)–O(1)	94.0(1)
Cu(1)–O(1)	1.918(3)	N(2)–Cu(1)–O(1*)	90.98(9)
Cu(1)–O(1*)	1.945(2)	O(1)–Cu(1)–O(1*)	80.50(9)
Cu(1)···Cu(1*)	2.949(1)	Cu(1)–O(1)–Cu(1*)	99.63(9)
O(1)···O(1*)	2.494(5)		

groups may become larger in the reaction with O<sub>2</sub> as discussed below. Despite our great efforts, single crystals of the copper(I) complex of <sup>Me</sup>Py<sup>1</sup><sup>Et,Bz-d2</sup> suitable for X-ray analysis could not be obtained so far.

**Dioxygen Reactivity of Copper(I) Complexes with <sup>H</sup>Py<sup>1</sup><sup>Et,Bz</sup> and <sup>Me</sup>Py<sup>1</sup><sup>Et,Bz</sup>.** As stated above, we have already demonstrated that oxygenation of the copper(I) complexes supported by bidentate ligands <sup>H</sup>Py<sup>1</sup><sup>Et,R3</sup> (R<sup>3</sup> = Bz or Phe) affords the bis-(μ-oxo)dicopper(III) complexes at a low temperature (Scheme 3).<sup>18–20</sup> For example, [Cu<sup>I</sup>(<sup>H</sup>Py<sup>1</sup><sup>Et,Bz-d2</sup>)(CH<sub>3</sub>CN)]PF<sub>6</sub> readily reacted with O<sub>2</sub> in a 2:1 ratio at −94 °C in acetone to give an ESR-silent bis-(μ-oxo)dicopper(III) complex exhibiting a characteristic absorption band at 400 nm [ $\epsilon = 17\,400\text{ M}^{-1}\text{ cm}^{-1}$ , spectrum (B) in Figure 2] together with a resonance Raman band at 606 cm<sup>−1</sup> (with <sup>16</sup>O<sub>2</sub>) that shifted to 577 cm<sup>−1</sup> upon <sup>18</sup>O<sub>2</sub> substitution (B in Scheme 5).<sup>19,20</sup>

When the bidentate ligand <sup>H</sup>Py<sup>1</sup><sup>Et,Bz-d2</sup> was replaced by <sup>Me</sup>Py<sup>1</sup><sup>Et,Bz-d2</sup>, which has the 6-methyl group on the pyridine nucleus, the oxygenated product of [Cu<sup>I</sup>(<sup>Me</sup>Py<sup>1</sup><sup>Et,Bz-d2</sup>)(CH<sub>3</sub>CN)]PF<sub>6</sub> was found to be totally different from that derived from [Cu<sup>I</sup>(<sup>H</sup>Py<sup>1</sup><sup>Et,Bz-d2</sup>)(CH<sub>3</sub>CN)]PF<sub>6</sub> under the same experimental conditions. The copper(I) complex of <sup>Me</sup>Py<sup>1</sup><sup>Et,Bz-d2</sup> reacts with dioxygen at −94 °C in acetone to afford the product which exhibits an absorption band at 365 nm ( $\epsilon = 17\,900\text{ M}^{-1}\text{ cm}^{-1}$ ) together with a weak band at 518 nm (860 M<sup>−1</sup> cm<sup>−1</sup>)

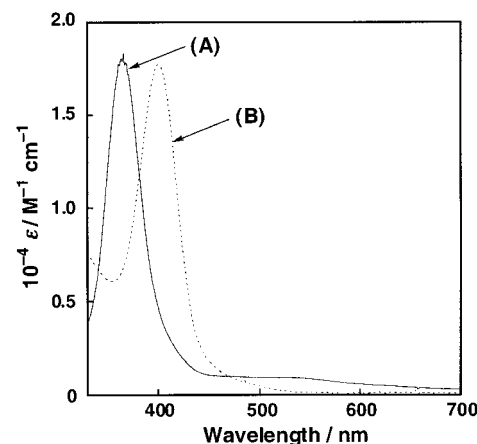


**Figure 2.** UV-vis spectra of the (μ-η<sup>2</sup>:η<sup>2</sup>-peroxo)dicopper(II) complex [(<sup>Me</sup>Py<sup>1</sup><sup>Et,Bz-d2</sup>)(Cu<sup>II</sup>)<sub>2</sub>(μ-O<sub>2</sub>)<sup>2+</sup>] (A) and the bis(μ-oxo)dicopper(III) complex [(<sup>H</sup>Py<sup>1</sup><sup>Et,Bz-d2</sup>)(Cu<sup>III</sup>)<sub>2</sub>(μ-O<sub>2</sub>)<sup>2+</sup>] (B) in acetone at −94 °C.

[spectrum (A) in Figure 2]. Such an absorption spectrum of the oxygenated product is reminiscent of formation of a side-on peroxo dicopper(II) complex. The resonance Raman spectrum of the oxygenated compound excited at 364.8 nm gave resonance enhanced peaks at 737 and 284 cm<sup>−1</sup> (with <sup>16</sup>O<sub>2</sub>), the former of which shifted to 696 cm<sup>−1</sup> upon <sup>18</sup>O<sub>2</sub>-substitution as demonstrated by the <sup>16</sup>O–<sup>18</sup>O difference spectrum (Figure 3, lower) and was assigned to the O–O stretching mode of the side-on peroxo ligand.<sup>4,5,13–15</sup> The Raman band around 280–290 cm<sup>−1</sup> has recently been assigned to an A<sub>g</sub> “breathing” mode of the Cu<sub>2</sub>O<sub>2</sub> peroxo core involving predominantly Cu–Cu stretching motion.<sup>22</sup> The stoichiometry of the reaction was determined as Cu:O<sub>2</sub> = 2:1 (±0.05), and the resulting solution was also ESR silent. These results unambiguously confirmed that the Cu<sub>2</sub>O<sub>2</sub> intermediate had a μ-η<sup>2</sup>:η<sup>2</sup>-peroxo bridge as illustrated in Scheme 5. Thus, introduction of just a methyl group into the 6-position of the pyridine nucleus of the bidentate ligand drastically alters the reactivity of the copper(I) complex toward O<sub>2</sub>, and this is the first example of quantitative formation of the (μ-η<sup>2</sup>:η<sup>2</sup>-peroxo)dicopper(II) complex (A) using a bidentate ligand.<sup>23</sup>

(22) Henson, M. J.; Mahadevan, V.; Stack, T. D. P.; Solomon, E. I. *Inorg. Chem.* **2001**, *40*, 5068–5069.



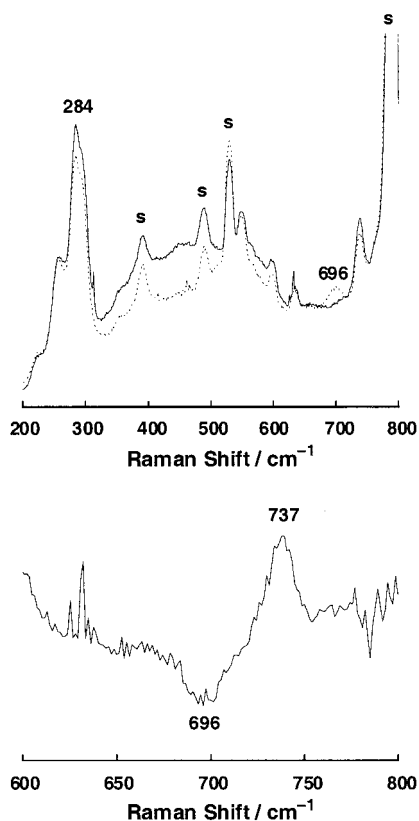


**Figure 3.** Resonance Raman spectra of  $[\{(\text{MePy}1^{\text{Et,Bz-d2}})(\text{Cu}^{\text{II}})\}_2(\mu\text{-}^{16}\text{O}_2)]^{2+}$  (solid line) and  $[\{(\text{MePy}1^{\text{Et,Bz-d2}})(\text{Cu}^{\text{II}})\}_2(\mu\text{-}^{18}\text{O}_2)]^{2+}$  (dashed line) in acetone at  $-100\text{ }^\circ\text{C}$  excited at 363.8 nm; “s” denotes a solvent band (upper) and a difference spectrum between the  $^{16}\text{O}$  and the  $^{18}\text{O}$  derivatives in the O–O stretching region (lower).

The  $(\mu\text{-}\eta^2\text{-}\eta^2\text{-peroxo})\text{dicopper(II)}$  complexes generated by using  $\text{MePy}1^{\text{Et,Bz}}$  and  $\text{MePy}1^{\text{Et,Bz-d2}}$  decomposed gradually to afford the oxidative N-dealkylation products, benzaldehyde and *N*-ethyl-2-(6-methylpyridin-2-yl)-ethylamine (see Experimental Section). The decomposition rates were determined from the decay of the absorption band at 365 nm due to the peroxo complex at various temperatures. The rates obeyed first-order kinetics, and the logarithm of the first-order rate constants ( $\log k_{\text{obs}}$ ) is plotted against  $1/T$  to give the Eyring plots as shown in Figure 4A. The kinetic isotope effect (KIE) is relatively small as 3.5 at  $-80\text{ }^\circ\text{C}$  that can be extrapolated to 1 at  $-16\text{ }^\circ\text{C}$  as shown in Figure 4A (the cross point of the two lines). Furthermore, the activation parameters determined from the Eyring plots in Figure 4A ( $\Delta H_{\text{H}}^\ddagger = 7.5 \pm 0.1\text{ kcal mol}^{-1}$ ,  $\Delta S_{\text{H}}^\ddagger = -28.9 \pm 0.5\text{ cal K}^{-1}\text{ mol}^{-1}$ ,  $\Delta H_{\text{D}}^\ddagger = 9.8 \pm 0.6\text{ kcal mol}^{-1}$ ,  $\Delta S_{\text{D}}^\ddagger = -20.1 \pm 3.4\text{ cal K}^{-1}\text{ mol}^{-1}$ ) are fairly close to those reported for the aliphatic ligand hydroxylation in the  $(\mu\text{-}\eta^2\text{-}\eta^2\text{-peroxo})\text{dicopper(II)}$  complex supported by the tridentate ligand  $\text{Py}2^{\text{Phe(-d4)}}$  (KIE = 1.8 at  $-40\text{ }^\circ\text{C}$ , 5.9 at  $-80\text{ }^\circ\text{C}$ ,  $\Delta H_{\text{H}}^\ddagger = 6.7 \pm 0.2\text{ kcal mol}^{-1}$ ,  $\Delta S_{\text{H}}^\ddagger = -37.0 \pm 0.7\text{ cal K}^{-1}\text{ mol}^{-1}$ ,  $\Delta H_{\text{D}}^\ddagger = 9.6 \pm 0.2\text{ kcal mol}^{-1}$ ,  $\Delta S_{\text{D}}^\ddagger = -25.6 \pm 0.7\text{ cal K}^{-1}\text{ mol}^{-1}$ ) (Scheme 2).<sup>13</sup> Such a small KIE (3.5 at  $-80\text{ }^\circ\text{C}$ ) and the disappearance of KIE (=1) at the higher temperature ( $-16\text{ }^\circ\text{C}$ ) could be interpreted by the mechanism that is similar to that proposed for the aliphatic ligand hydroxylation in the  $(\mu\text{-}$

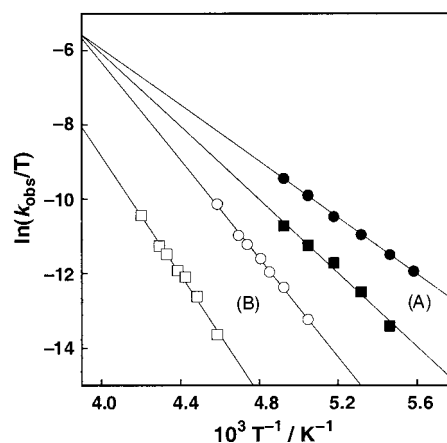


**Figure 4.** Eyring plots for the decomposition process of (A)  $[\{(\text{MePy}1^{\text{Et,Bz-d2}})(\text{Cu}^{\text{II}})\}_2(\mu\text{-O}_2)]^{2+}$  (●) and  $[\{(\text{MePy}1^{\text{Et,Bz}})(\text{Cu}^{\text{II}})\}_2(\mu\text{-O}_2)]^{2+}$  (■) and (B)  $[\{(\text{HPy}1^{\text{Et,Bz-d2}})(\text{Cu}^{\text{III}})\}_2(\mu\text{-O}_2)]^{2+}$  (○) and  $[\{(\text{HPy}1^{\text{Et,Bz}})(\text{Cu}^{\text{III}})\}_2(\mu\text{-O}_2)]^{2+}$  (□).

$\eta^2\text{-}\eta^2\text{-peroxo})\text{dicopper(II)}$  complex supported by  $\text{Py}2^{\text{Phe(-d4)}}$  (Scheme 2).<sup>13</sup> Thus, the  $(\mu\text{-}\eta^2\text{-}\eta^2\text{-peroxo})\text{dicopper(II)}$  species (A) is not the actual active oxygen intermediate for the benzylic C–H bond activation (the initial step of the oxidative N-dealkylation), but O–O bond homolysis of the peroxo intermediate would occur prior to the following C–H bond activation process. If the O–O bond homolysis is solely the rate-determining step, the KIE value would be 1.0. The observed small KIE values suggest that the O–O bond homolysis ( $k_{\text{h}}$ ) is much slower than the back reaction ( $k_{-\text{h}}$ ) which competes with the facile C–H bond activation ( $k_{\text{CH}}$ ). In such a case, the observed rate constant  $k$  is given by equation  $k = k_{\text{h}}k_{\text{CH}}/(k_{-\text{h}} + k_{\text{CH}})$ . The O–O bond homolysis may be largely the rate-determining step, that is,  $k_{\text{CH}} \gg k_{-\text{h}}$ , but the ligand deuteration may result in a significant decrease in the rate of the C–D cleavage ( $k_{\text{CD}}$ ), which becomes partially rate-determining.

Decomposition of the bis( $\mu\text{-oxo})\text{dicopper(III)}$  complex derived from  $\text{HPy}1^{\text{Et,Bz}}$  or  $\text{HPy}1^{\text{Et,Bz-d2}}$  which has no 6-methyl group on the pyridine nucleus also led to oxidative N-dealkylation reaction of the benzyl group. In this case, however, a very large kinetic deuterium isotope effect (KIE) of 32.9 (at  $-55\text{ }^\circ\text{C}$ ) was obtained. Such a large KIE value and the activation parameters ( $\Delta H_{\text{H}}^\ddagger = 13.1 \pm 0.2\text{ kcal mol}^{-1}$ ,  $\Delta S_{\text{H}}^\ddagger = -7.3 \pm 1.1\text{ cal K}^{-1}\text{ mol}^{-1}$ ,  $\Delta H_{\text{D}}^\ddagger = 15.9 \pm 0.6\text{ kcal mol}^{-1}$ ,  $\Delta S_{\text{D}}^\ddagger = -1.3 \pm 2.7\text{ cal K}^{-1}\text{ mol}^{-1}$ ) determined from the Eyring plots shown in Figure 4B are similar to those reported for the aliphatic ligand hydroxylation in the bis( $\mu\text{-oxo})\text{dicopper(III)}$  core supported by  $\text{HPy}1^{\text{Et,Phe(-d4)}}$  ( $\Delta H_{\text{H}}^\ddagger = 9.3 \pm 0.1\text{ kcal mol}^{-1}$ ,  $\Delta S_{\text{H}}^\ddagger = -17.4 \pm 0.5\text{ cal K}^{-1}\text{ mol}^{-1}$ ,  $\Delta H_{\text{D}}^\ddagger = 12.6 \pm 0.1\text{ kcal mol}^{-1}$ ,  $\Delta S_{\text{D}}^\ddagger = -7.4 \pm 0.5\text{ cal K}^{-1}\text{ mol}^{-1}$ ) (Scheme 3).<sup>18</sup> This indicates that the oxidative N-dealkylation reaction proceeds via a similar mechanism: rate-determining hydrogen atom abstraction and oxygen rebound or its concerted variant as stated above.

The  $(\mu\text{-}\eta^2\text{-}\eta^2\text{-peroxo})\text{dicopper(II)}$  and bis( $\mu\text{-oxo})\text{dicopper(III)}$  complexes are known to have similar thermodynamic stability such that changes in ligand substituents as well as solvent and/or counteranion are sufficient to result in formation of one or the other form.<sup>23–27</sup> Steric repulsion between the bulky substit-

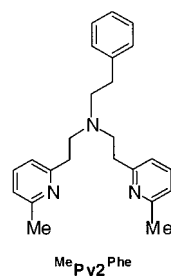
(23) A mixture of the  $(\mu\text{-}\eta^2\text{-}\eta^2\text{-peroxo})\text{dicopper(II)}$  and bis( $\mu\text{-oxo})\text{dicopper(III)}$  complexes has been obtained in the reaction of copper(I) complex of *N,N'*-dimethyl-*N,N'*-di-*tert*-butylethylenediamine bidentate ligand with  $\text{O}_2$ . Mahadevan, V.; Henson, M. J.; Solomon, E. I.; Stack, T. D. P. *J. Am. Chem. Soc.* **2000**, *122*, 10249–10250.

(24) Tolman, W. B. *Acc. Chem. Res.* **1997**, *30*, 227–237.

(25) Mahapatra, S.; Halfen, J. A.; Wilkinson, E. C.; Pan, G.; Cramer, C. J.; Que, L., Jr.; Tolman, W. B. *J. Am. Chem. Soc.* **1995**, *117*, 8865–8866.

(26) Halfen, J. A.; Mahapatra, S.; Wilkinson, E. C.; Kaderli, S.; Young, V. G., Jr.; Que, L., Jr.; Zuberbühler, A. D.; Tolman, W. B. *Science* **1996**, *271*, 1397–1400.

Chart 3



uents of the capping ligands as well as the interaction between the  $\text{Cu}_2\text{O}_2$  core and solvent and/or counteranion have been invoked as the major factors that control the equilibrium position between the two species, although the mechanistic details of their functions have yet to be clearly understood.

The selective formation of the ( $\mu$ - $\eta^2$ : $\eta^2$ -peroxy)dicopper(II) complex (**A**) using the bidentate ligand ( $\text{MePy1}^{\text{Et,Bz}}$ ) can be explained by the steric effect of the 6-methyl group of the pyridine nucleus. The bis( $\mu$ -oxo)dicopper(III) complex (**B**) requires a shorter Cu–N<sub>py</sub> distance ( $\sim 1.9$  Å) than the ( $\mu$ - $\eta^2$ : $\eta^2$ -peroxy)dicopper(II) complex (**A**) ( $\sim 2.0$  Å).<sup>28,29</sup> The steric repulsion between the 6-methyl group and the metal center may inhibit the  $\text{Cu}_2\text{O}_2$  complex of  $\text{MePy1}^{\text{Et,Bz}}$  to adapt to such a shorter Cu–N<sub>py</sub> distance, enforcing the equilibrium strongly toward the peroxy species.<sup>30</sup> The donor ability of the pyridine nitrogen is also reduced by the steric effect of the 6-methyl group,<sup>31</sup> destabilizing the higher oxidation state of the metal centers in the bis( $\mu$ -oxo) species. Such steric and/or electronic effects of the 6-methyl group have recently been reported in the tridentate ligand system.<sup>32</sup> Introduction of just a methyl group into the 6-position of the pyridine nuclei to give  $\text{MePy2}^{\text{Phe}}$  (Chart 3) induces strong binding of MeCN to copper(I) in the cuprous complex, resulting in loss of its reactivity toward dioxygen.<sup>32</sup> The 6-methyl group may prevent the cuprous complex to adopt three-coordinate geometry with a shorter Cu–N<sub>py</sub> distance that is required for the ligand exchange between MeCN and  $\text{O}_2$ .

#### Dioxygen Reactivity of Copper(I) Complex with $\text{HPy1}^{\text{Me,Me}}$ .

Four-electron reduction of dioxygen to water is accomplished at a trinuclear copper active center in multi-copper enzymes such as ascorbate oxidase, laccase, and ceruloplasmin.<sup>6</sup> A trinuclear copper site has also been invoked as the reaction center of particulate methane monooxygenase (pMMO), which catalyzes hydroxylation of methane to methanol.<sup>33</sup> Despite such

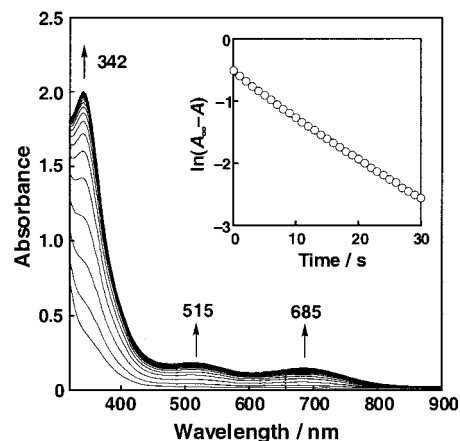


**Figure 5.** Spectral change observed upon introduction of  $\text{O}_2$  gas into an acetone solution of  $[\text{Cu}^{\text{I}}(\text{HPy1}^{\text{Me,Me}})(\text{CF}_3\text{SO}_3)]$  ( $5.0 \times 10^{-3}$  M) at  $-94$  °C. Inset: First-order plot based on the absorbance change at 515 nm.

important roles of the trinuclear copper active sites in biological dioxygen processing, there has been a limited number of model compounds of trinuclear copper/dioxygen complexes reported so far.<sup>21,34</sup> Stack and co-workers have demonstrated that the copper(I) complex of a bidentate ligand,  $N,N,N',N'$ -tetramethyl-*trans*-cyclohexanediamine, reacts with molecular oxygen in a 3:1 ratio at a relatively high concentration ( $> 10$  mM) of the copper(I) complex to give a mixed-valence trinuclear copper(II, II, III) complex with two  $\mu_3$ -oxo bridges.<sup>21</sup> This reaction models the four-electron reduction of dioxygen at the trinuclear copper active site in the enzymes and provides another possible reaction pattern in copper(I)-dioxygen chemistry in model systems. However, the formation mechanism and reactivity of the trinuclear copper complex have yet to be elucidated. In this study, the bidentate ligand with the smallest *N*-alkyl substituents,  $\text{HPy1}^{\text{Me,Me}}$ , has been adopted to clarify the formation mechanism and reactivity of the mixed-valence trinuclear copper(II, II, III) complex.

Treatment of a 5.0 mM acetone solution of  $[\text{Cu}^{\text{I}}(\text{HPy1}^{\text{Me,Me}})(\text{CF}_3\text{SO}_3)]$  with dioxygen at  $-94$  °C resulted in color change of the solution from pale yellow to dark brown. A typical example of the spectral change for the oxygenation reaction of  $[\text{Cu}^{\text{I}}(\text{HPy1}^{\text{Me,Me}})(\text{CF}_3\text{SO}_3)]$  is shown in Figure 5 (measured by using a 1 mm path length UV cell), where a strong absorption band at 342 nm ( $\epsilon = 12\,000$   $\text{M}^{-1} \text{cm}^{-1}$ ) together with two small bands at 515 (1000) and 685 nm ( $800$   $\text{M}^{-1} \text{cm}^{-1}$ ) rapidly developed. The final spectrum of the reaction is significantly different from that of the bis( $\mu$ -oxo)dicopper(III) complex ( $\lambda_{\text{max}} = 400$  nm,  $\epsilon = 17\,400$   $\text{M}^{-1} \text{cm}^{-1}$ ) generated in the reaction of copper(I) complex with bulkier bidentate ligand such as  $[\text{Cu}^{\text{I}}(\text{HPy1}^{\text{Et,Bz-d2}})(\text{CH}_3\text{CN})]\text{PF}_6$  with  $\text{O}_2$  in acetone [spectrum (**B**) in Figure 2], but is fairly close to that of the bis( $\mu_3$ -oxo)-trinuclear copper(II, II, III) complex reported by Stack et al. [ $\lambda_{\text{max}} = 355$  (15 000), 480 (1400), and 620 nm ( $800$   $\text{M}^{-1} \text{cm}^{-1}$ )].<sup>21</sup> Stoichiometry of Cu: $\text{O}_2$  of the reaction has been determined by manometry as 3:1 ( $\pm 0.05$ ). Furthermore, the acetone solution of the oxygenated intermediate was ESR silent. These features of the oxygenated intermediate, being quite similar to those of the reported trinuclear mixed valence copper(II, II, III) bis( $\mu_3$ -oxo) complex, strongly indicate formation of the same type of intermediate in the present  $\text{HPy1}^{\text{Me,Me}}$  system (Scheme 6).

(27) Cahoy, J.; Holland, P. L.; Tolman, W. B. *Inorg. Chem.* **1999**, *38*, 2161–2168.

(28) Mahapatra, S.; Halfen, J. A.; Wilkinson, E. C.; Pan, G.; Wang, X.; Young, V. G., Jr.; Cramer, C. J.; Que, L., Jr.; Tolman, W. B. *J. Am. Chem. Soc.* **1996**, *118*, 11555–11574.

(29) Kitajima, N.; Fujisawa, K.; Fujimoto, C.; Moro-oka, Y.; Hashimoto, S.; Kitafawa, T.; Toriumi, K.; Tatsumi, K.; Nakamura, A. *J. Am. Chem. Soc.* **1992**, *114*, 1277–1291.

(30) Interaction between two 6-methylpyridines and the copper(III) ion in the Suzuki's bis( $\mu$ -oxo)dicopper(III) complex supported by bis[(6-methylpyridin-2-yl)methyl](2-pyridinylmethyl)amine ( $\text{Me}_2\text{TPA}$ ) is known to be very weak (Cu–NMePy: 2.48, 2.55 Å), while the remaining pyridine without the substituent strongly bound to the metal center (Cu–NPy: 1.91 Å) to stabilize the copper(III) state. See: Hayashi, H.; Fujinami, S.; Nagatomo, S.; Ogo, S.; Suzuki, M.; Uehara, A.; Watanabe, Y.; Kitagawa, T. *J. Am. Chem. Soc.* **2000**, *122*, 2124–2125.

(31) Nagao, H.; Komeda, N.; Mukaida, M.; Suzuki, M.; Tanaka, K. *Inorg. Chem.* **1996**, *35*, 6809–6815.

(32) Osako, T.; Tachi, Y.; Taki, M.; Fukuzumi, S.; Itoh, S. *Inorg. Chem.* **2001**, *40*, 6604–6609.

(33) Chan, S. I.; Nguyen, H. T.; Shiemke, A. K.; Lidstrom, M. E. In *Bioinorganic Chemistry of Copper*; Karlin, K. D., Tyeklár, Z., Eds.; Chapman & Hall: New York, 1993; pp 184–195.

(34) Karlin, K. D.; Gan, Q.-F.; Farooq, A.; Liu, S.; Zubieta, J. *Inorg. Chem.* **1990**, *29*, 2549–2551.

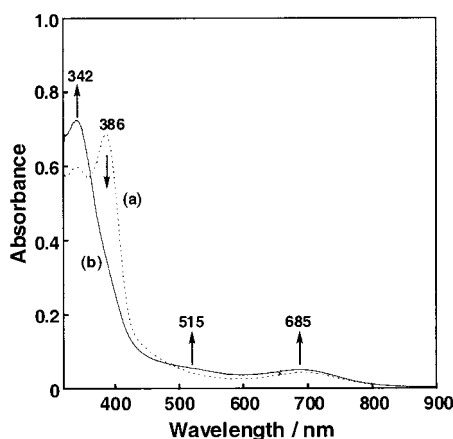
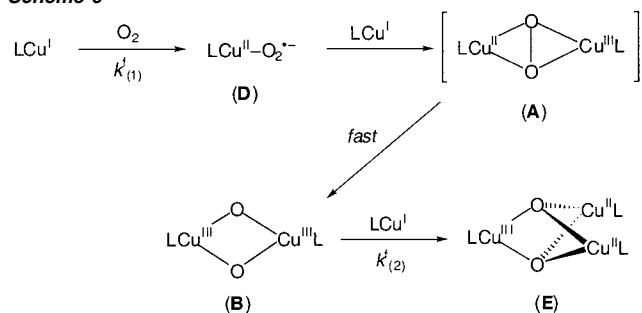


**Figure 6.** UV-vis spectrum obtained upon addition of O<sub>2</sub> gas into an acetone solution of [Cu<sup>I</sup>(<sup>H</sup>Py1<sup>Me,Me</sup>)(CF<sub>3</sub>SO<sub>3</sub>)] (0.2 × 10<sup>-3</sup> M) at -94 °C (A, dashed line) and that obtained after another addition of [Cu<sup>I</sup>(<sup>H</sup>Py1<sup>Me,Me</sup>)(CF<sub>3</sub>SO<sub>3</sub>)] (0.1 × 10<sup>-3</sup> M) under anaerobic conditions (before the addition of the copper(I) complex Ar gas was bubbled for 15 min) (B, solid line).

#### Scheme 6



The formation rate of the bis( $\mu_3$ -oxo) trinuclear copper complex (E) obeys first-order kinetics as shown in the inset of Figure 5. The first-order dependence of the formation process has also been confirmed by the fact the pseudo-first-order-rate constants ( $k_{\text{obs}}^f$ ; the suffix “f” denotes “formation process”) are nearly the same within an experimental error when the concentration of the starting copper(I) complex is changed from 3.0 to 8.0 mM ( $k_{\text{obs}}^f = 5.9 (\pm 0.2) \times 10^{-2} \text{ s}^{-1}$ ). The first-order kinetics have clearly indicated that the primary reaction between the copper(I) complex (starting material) and dioxygen to form a mononuclear copper(II)-superoxo intermediate (D in Scheme 6) is the rate-determining step ( $k_{\text{obs}}^f = k_{(1)}^f$ ), and the subsequent steps, D to B through A and B to E, are much faster. In contrast, the oxygenation reaction of the copper(I) complex of <sup>H</sup>Py1<sup>Et,Bz-d2</sup>, that is, the formation of the bis( $\mu$ -oxo)dicopper(III) (B), followed the second-order rate law.<sup>18</sup> This indicates that the reaction of superoxo-copper(II) intermediate D and the copper(I) complex is rate-limiting in the <sup>H</sup>Py1<sup>Et,Bz-d2</sup> system. The bulkier N-substituents in <sup>H</sup>Py1<sup>Et,Bz-d2</sup> may retard the self-assembling dimerization reaction (D to A), whereas the small methyl group in <sup>H</sup>Py1<sup>Me,Me</sup> may not.

When the reaction was carried out at a lower concentration of the copper(I) complex such as 0.2 mM, a different spectrum was obtained as shown in Figure 6 [spectrum (a)], where coexistence of a bis( $\mu$ -oxo)dicopper(III) complex with the trinuclear copper complex was implicated by the appearance of a characteristic absorption band at 386 nm together with the bands due to the trinuclear copper complex. In fact, the solution gave a resonance Raman band at 628 cm<sup>-1</sup> with <sup>16</sup>O<sub>2</sub> that shifted to 594 cm<sup>-1</sup> upon <sup>18</sup>O<sub>2</sub> substitution (Figure S1). The isotope

sensitive Raman bands around 600 cm<sup>-1</sup> in copper/dioxygen chemistry are now well recognized as diagnostic for formation of the bis( $\mu$ -oxo)dicopper(III) complex.<sup>35,36</sup> Interestingly enough, addition of another 0.1 mM acetone solution of [Cu<sup>I</sup>(<sup>H</sup>Py1<sup>Me,Me</sup>)(SO<sub>3</sub>CF<sub>3</sub>)] into the mixture under anaerobic conditions (Ar gas was bubbled for 15 min before the additional addition of copper(I) complex) resulted in a decrease of the absorption band at 386 nm due to the bis( $\mu$ -oxo)dicopper(III) complex together with an increase of the bands at 342, 515, and 685 nm due to the trinuclear copper(II, II, III) complex as depicted in Figure 6 [spectrum (b)]. Thus, the bis( $\mu$ -oxo)dicopper(III) complex in the mixture is converted into the bis( $\mu_3$ -oxo) trinuclear copper(II, II, III) species by the reaction with the copper(I) starting material. This indicates that the former is the precursor of formation of the later as indicated in Scheme 6. At higher concentration of the copper(I) starting material (mM order), the reaction between the bis( $\mu$ -oxo)dicopper(III) intermediate (B) and another molecule of copper(I) may be fast enough to generate the trinuclear complex predominantly. On the other hand, at the lower copper(I) concentration, there is not enough copper(I) complex remaining in the solution for the complete conversion of B to E. Thus, the reaction at the lower concentration gave a mixture of the two species (B and E). Further addition of the copper(I) complex to the mixture under Ar resulted in conversion of the coexisting bis( $\mu$ -oxo)dicopper(III) complex (B) to the trinuclear complex (E) as depicted in Figure 6. From the spectral change shown in Figure 6 was determined the second-order rate constant  $k_{(2)}^f$  for the reaction between B and the copper(I) complex as  $3.4 (\pm 0.2) \times 10^2 \text{ M}^{-1} \text{ s}^{-1}$  at -94 °C.

As suggested by the crystal structures of the copper(I)-phosphine complexes (Figure 1), steric bulkiness of the N-alkyl substituents in <sup>H</sup>Py1<sup>R2,R3</sup> is the major factor that controls the reactivity of the copper complexes. In fact, ligand <sup>H</sup>Py1<sup>Et,Bz-d2</sup> afforded predominantly the bis( $\mu$ -oxo)dicopper(III) complex even at the higher concentration (3.0 mM) of the starting copper(I) complex under otherwise the same reaction conditions (Figure S2). Thus, the N-substituents of the bidentate ligand significantly alter the copper(I)-dioxygen reactivity.

**Reactivity of the Bis( $\mu_3$ -oxo) Trinuclear Copper(II, II, III) Complex.** The bis( $\mu_3$ -oxo) trinuclear copper(II, II, III) complex E (1.7 mM) reacted with 2,4-di-*tert*-butylphenol (DBP, 10 mM) in acetone at -80 °C to give 3,5,3',5'-tetra-*tert*-butyl-biphenyl-2,2'-diol (C-C coupling dimer) as the oxidation product. <sup>1</sup>H NMR spectrum of the organic product mixture obtained by extraction of the final reaction mixture with ether has indicated that the yield of the C-C coupling dimer is 97% based on the trinuclear complex used. This unambiguously indicates that the copper(II, II, III) complex E acts formally as a two-electron oxidant. When the final reaction mixture was allowed to stand for several hours, single crystals of a product derived from the copper complex were obtained, for which X-ray crystallographic analysis has also been carried out. The crystal structure of the product is shown in Figure 7 together with the crystallographic data and the selected bond lengths and angles in Tables 1 and 2, respectively. It is a bis( $\mu$ -hydroxo)dicopper(II) complex, [Cu<sup>II</sup><sub>2</sub>(<sup>H</sup>Py1<sup>Me,Me</sup>)<sub>2</sub>( $\mu$ -OH)<sub>2</sub>](CF<sub>3</sub>SO<sub>3</sub>)<sub>2</sub> (F), having an imposed

- (35) Holland, P. L.; Cramer, C. J.; Wilkinson, E. C.; Mahapatra, S.; Rodgers, K. R.; Itoh, S.; Taki, M.; Fukuzumi, S.; Que, L., Jr.; Tolman, W. B. *J. Am. Chem. Soc.* **2000**, *122*, 792–802.  
 (36) Henson, M. J.; Mukherjee, P.; Root, D. E.; Stack, T. D. P.; Solomon, E. I. *J. Am. Chem. Soc.* **1999**, *121*, 10332–10345.



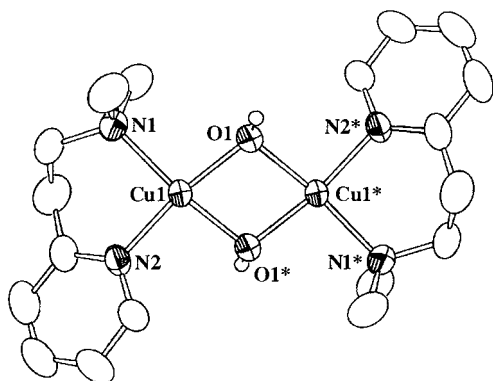


**Figure 7.** ORTEP drawing of the cationic parts of  $[\text{Cu}^{\text{II}}_2(\text{HPy}^{\text{Me,Me}})_2(\mu\text{-OH})_2](\text{CF}_3\text{SO}_3)_2$  showing 50% probability thermal-ellipsoid. Hydrogen atoms except the hydroxyl H and counteranions are omitted for clarity.

center of symmetry in the  $\text{Cu}_2\text{O}_2$  core. Each copper ion exhibits a square planar geometry which consists of a  $\text{N}_2\text{O}_2$  donor set provided from the bidentate ligands and the bridging OH groups. The complex **F** was ESR silent due to strong magnetic interaction between the two cupric ions through the *m*-hydroxo bridges. Because the  $\text{Cu}-\text{O}-\text{Cu}$  angle in **F** is  $99.63(9)^\circ$  (see Table 2), the magnetic interaction is antiferromagnetic. Crawford et al. have established the linear correlation between the  $\text{Cu}-\text{O}-\text{Cu}$  angle ( $\theta$ ) of a series of bis( $\mu$ -hydroxo)dicopper(II) complexes and their singlet–triplet exchange parameter as  $J = -74.53\theta + 7270 \text{ cm}^{-1}$ .<sup>37</sup> From this correlation, it can be concluded that when  $\theta$  is larger than  $97.55^\circ$ , the overall magnetic behavior is antiferromagnetic. Complex **F** exhibits absorption bands at 355 nm ( $\epsilon = 1400 \text{ M}^{-1} \text{ cm}^{-1}$ ) and 595 nm ( $\epsilon = 180 \text{ M}^{-1} \text{ cm}^{-1}$ ), the latter of which is used to estimate the yield of the dicopper(II) complex in a UV–vis scale reaction (vide infra).

In Figure 8A is shown the spectral change observed upon addition of DBP ( $1.0 \times 10^{-2} \text{ M}$ ) to an acetone solution of complex **E** ( $1.0 \times 10^{-3} \text{ M}$ ) at  $-90^\circ \text{C}$ , where the characteristic absorption bands at 515 and 685 nm due to **E** decrease to attain spectrum (a) exhibiting a  $\lambda_{\text{max}}$  at 570 nm.<sup>38</sup> The time course of the absorption change obeys first-order kinetics, and the pseudo-first-order rate constant ( $k^{\text{r}}_{\text{obs}(1)}$ ; the suffix “r” denotes “reaction”) increases linearly with increasing substrate concentration as shown in the inset of Figure 8A. From the slope of the linear line was determined the second-order rate constant  $k^{\text{r}}_{(1)}$  as  $0.46 \pm 0.02 \text{ M}^{-1} \text{ s}^{-1}$  at  $-90^\circ \text{C}$ .

When the same reaction was carried out at  $-70^\circ \text{C}$  [Figure 8B], the absorption bands due to **E** (515 and 685 nm) rapidly changed to the spectrum (a), which further changed slowly to the spectrum (b) that is exactly the same as the spectrum of bis( $\mu$ -hydroxo)dicopper(II) complex **F** ( $\lambda_{\text{max}} = 595 \text{ nm}$ ). Judging from the absorption intensity at 595 nm of the final spectrum (b), the amount of **F** formed in this reaction is nearly equal to that of the starting material **E**. In other words, one molecule of the bis( $\mu$ -hydroxo)dicopper(II) complex (**F**) is produced from one molecule of the trinuclear copper(II, II, III) complex (**E**). Thus, it is apparent that the reaction between **E** and DBP to give **F** and the C–C coupling dimer proceeds stepwise through an intermediate **X** exhibiting the spectrum (a).

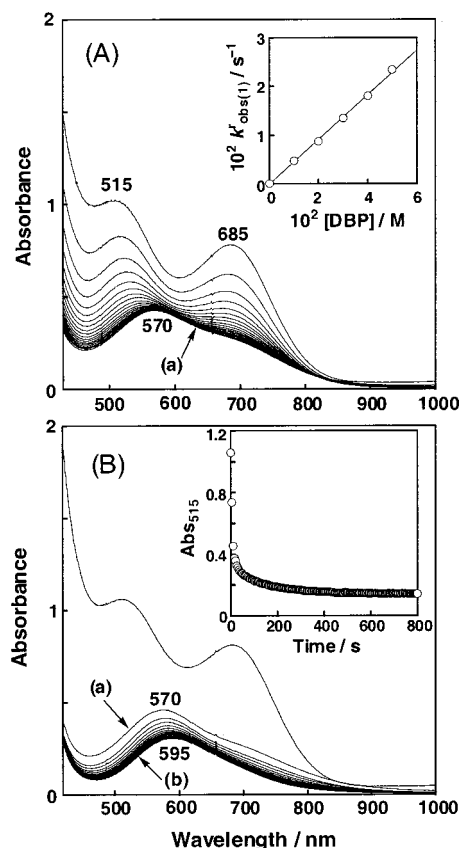


**Figure 8.** Spectral changes for (A) the first process of the reaction between complex **E** ( $1.0 \times 10^{-3} \text{ M}$ ) and DBP ( $1.0 \times 10^{-2} \text{ M}$ ) in acetone at  $-90^\circ \text{C}$  (Inset: Plot of  $k^{\text{r}}_{\text{obs}(1)}$  vs  $[\text{DBP}]$ ) and for (B) the reaction of **E** ( $1.0 \times 10^{-3} \text{ M}$ ) and DBP ( $7.0 \times 10^{-2} \text{ M}$ ) in acetone at  $-70^\circ \text{C}$  (Inset: Time course of the absorbance change at 515 nm); (a) the spectrum of intermediate **X** indicated in Scheme 7; (b) the final spectrum of the reaction that is exactly the same as that of the bis( $\mu$ -hydroxo)dicopper(II) complex (**F**).

The second slow process also obeys pseudo-first-order kinetics, but a plot of the pseudo-first-order rate constant  $k^{\text{r}}_{\text{obs}(2)}$  against the DBP concentration gave a Michaelis–Menten type saturation curve as shown in Figure S3. This implicates that the second slow process involves a complex formation between intermediate **X** and DBP to give another intermediate **Y**. From the double reciprocal plot shown in the inset of Figure S3 were determined the equilibrium constant  $K$  and the rate constant  $k^{\text{r}}_{(2)}$  as  $44.6 \pm 2.2 \text{ M}^{-1}$  and  $9.5 (\pm 0.5) \times 10^{-3} \text{ s}^{-1}$  at  $-70^\circ \text{C}$ , respectively.

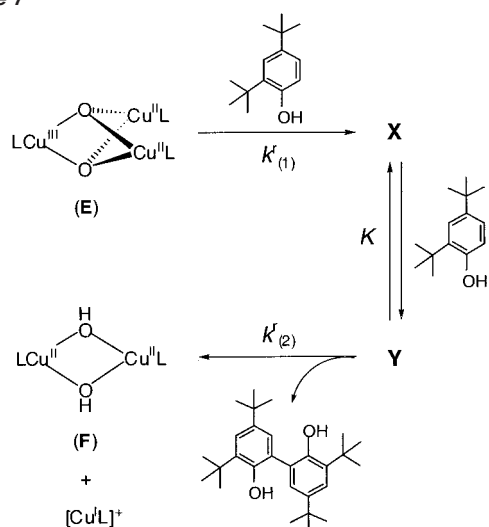
A possible mechanism for the reaction between **E** and DBP is illustrated in Scheme 7. In the first process, trinuclear copper(II, II, III) complex **E** reacts with DBP to give an intermediate **X**. The intermediate **X** exhibits an absorption band at 570 nm (spectrum (a) in Figure 8) which could be assigned to the d–d transitions of the copper(II) ions of the intermediate. Because no reaction took place when the sterically bulkiest phenol, 2,4,6-tri-*tert*-butylphenol (TBP), was used as the substrate instead of DBP, the first process with DBP may involve coordination of the phenol to one of the copper ion (probably copper(III) site) in the trinuclear copper(II, II, III) complex **E**. Although structural details about intermediate **X** have yet to be clarified, we presume that the three copper ions are still associated in the intermediate **X**, since no ESR active species is detected during the course of the reaction. The intermediate **X** then further reacts with another molecule of DBP to give an

(37) Drawford, V. H.; Richardson, H. W.; Wasson, J. R.; Hodgson, D. J.; Hatfield, W. E. *Inorg. Chem.* **1976**, *15*, 2107–2110.

(38) The trinuclear copper(II, II, III) complex (**E**) is fairly stable at the low temperature, so that self-decomposition of the complex is negligible below  $-70^\circ \text{C}$ .



Scheme 7



intermediate **Y**, from which one molecule of bis( $\mu$ -hydroxo)dicopper(II) complex **F** and the dimer product are released to complete the reaction (Scheme 7). Because the trinuclear copper(II, II, III) complex acts formally as a two-electron oxidant to give an equimolar amount of the dicopper(II) complex and the dimer product of DBP, 1 equiv of copper(I) complex should be released as indicated in Scheme 7. Although we could not estimate the yield of such colorless copper(I) complex by UV-vis, ESI-MS measurement did confirm the existence of copper(I) complex  $[\text{Cu}(\text{HPy}1^{\text{Me,Me}})]^+$  in the final reaction mixture. Importance of the coordinative interaction between the phenol substrate and the copper sites of intermediates is also implicated by the fact that 1,4-cyclohexadiene (CHD) having a similar weak C-H bond did not react with **E** under the same experimental conditions.<sup>39</sup>

## Conclusion

A series of simple bidentate ligands,  $\text{R}^1\text{Py}1^{\text{R}2,\text{R}3}$ , allowed us to assess three totally different copper-active oxygen complexes, ( $\mu$ - $\eta^2$ : $\eta^2$ -peroxo)dicopper(II) complex (**A**), bis( $\mu$ -oxo)dicopper(III) complex (**B**), and mixed-valence bis( $\mu_3$ -oxo) trinuclear copper(II, II, III) complex (**E**). The bidentate ligand with the 6-methyl substituent on the pyridine nucleus  $\text{MePy}1^{\text{Et,Bz}}$  predominantly provided the ( $\mu$ - $\eta^2$ : $\eta^2$ -peroxo)dicopper(II) complex (**A**), while the bidentate ligand without the 6-methyl group  $\text{HPy}1^{\text{Et,Bz}}$  afforded the bis( $\mu$ -oxo)dicopper(III) complex (**B**) under the same experimental conditions (Scheme 5). Such a drastic effect of the 6-methyl group on the  $\text{Cu}_2\text{O}_2$  intermediates has been interpreted by steric repulsion between the 6-methyl group and the metal center, which inhibits close approach of Cu to the nitrogen atom of the pyridine nucleus. Such a short distance of Cu-N is required for the formation of the high valent copper-oxo complex (**B**).<sup>28</sup> The donor ability of the nitrogen is also reduced by the steric effect of the 6-methyl group, destabilizing the bis( $\mu$ -oxo)dicopper(III) complex (**B**) in the  $\text{MePy}1^{\text{Et,Bz}}$  case. In the oxidative N-dealkylation reactions with the copper(I)

complexes of  $\text{MePy}1^{\text{Et,Bz}(-\text{d}2)}$  and  $\text{HPy}1^{\text{Et,Bz}(-\text{d}2)}$  with  $\text{O}_2$ , the KIE and the activation parameters have indicated that the bis( $\mu$ -oxo)dicopper(III) complex is a common intermediate for the intramolecular C-H bond activation of the ligand sidearm.

Adoption of the small *N*-alkyl substituents of the bidentate ligand and higher concentration of the starting material allows us to attain the trinuclear copper complex **E** via the reaction involving the copper(II)-superoxo and bis( $\mu$ -oxo)dicopper(III) intermediates (**D** and **B**) as shown in Scheme 6. The trinuclear copper(II, II, III) complex **E** supported by  $\text{HPy}1^{\text{Me,Me}}$  has been demonstrated to act as a two-electron oxidant in the reaction with the phenol substrate (Scheme 7). The two-oxidation ability of **E** has also been demonstrated in the reaction with  $\text{AcrH}_2$ .<sup>39</sup>

Recently, Solomon et al. and Sakurai et al. independently reported formation of a similar type of active oxygen intermediate in the oxygenation reaction of modified multi-copper oxidase (laccase) carrying three cuprous ions in the enzyme active site.<sup>40-42</sup> Although they proposed that the active oxygen intermediate involved a hydroperoxo or a peroxo structure, it is interesting to note that the UV-vis spectra of their active oxygen intermediates (Solomon's intermediate, 340, 470, and 680 nm; Sakurai's intermediate, 340, 475, and 680 nm) are very close in shape and peak positions to those of the trinuclear copper(II, II, III) complex reported here. Further model studies will be merited to provide structural information about the active oxygen intermediates of the multi-copper enzymes.

## Experimental Section

**General.** All chemicals used in this study except the ligands and the complexes were commercial products of the highest available purity and were further purified by the standard methods, if necessary.<sup>43</sup> 6-Methyl-2-vinylpyridine was kindly supplied by Koei Chemical Co. Ltd. and was purified by fractional distillation. FT-IR spectra were recorded with a Shimadzu FTIR-8200PC. UV-vis spectra were measured using a Hewlett-Packard HP8453 diode array spectrophotometer with a Unisoku thermostated cell holder designed for low-temperature measurements. Mass spectra were recorded with a JEOL JMS-700T Tandem MS station. ESI-MS (electrospray ionization mass spectra) measurements were performed on a PE SCIEX API 150EX.  $^1\text{H}$  NMR spectra were recorded on a JEOL FT-NMR Lambda 300WB. ESR measurements were performed on a JEOL JES-ME-2X spectrometer at  $-196^\circ\text{C}$  (liquid  $\text{N}_2$  temperature).

**Synthesis.**  $\text{HPy}1^{\text{Et,Bz}}$  (*N*-Benzyl-*N*-ethyl-2-(2-pyridyl)ethylamine). A mixture of benzylamine (2.14 g, 20 mmol), 2-vinylpyridine (2.10 g, 20 mmol), and acetic acid (1.20 g, 20 mmol) in methanol (70 mL) was refluxed for 40 h. After removal of the solvent by evaporation, the resulting residue was dissolved in  $\text{CH}_2\text{Cl}_2$  (100 mL), and the  $\text{CH}_2\text{Cl}_2$  solution was washed with 10% aqueous NaOH three times and dried over anhydrous  $\text{K}_2\text{CO}_3$ . After removal of  $\text{K}_2\text{CO}_3$  by filtration, evaporation of the organic solvent gave brown oily material, from which *N*-benzyl-2-(2-pyridyl)ethylamine was isolated by  $\text{SiO}_2$  column chromatography ( $\text{CHCl}_3$ -AcOEt) in 72% yield.  $^1\text{H}$  NMR (270 MHz,  $\text{CDCl}_3$ ):  $\delta$  3.00–3.07 (m, 4H,  $-\text{CH}_2-\text{CH}_2-\text{Py}$ ), 3.83 (s, 2H,  $-\text{CH}_2-\text{Ph}$ ), 7.12 (1H, d,  $J = 5.4$  Hz,  $\text{H}_{\text{py}-3}$ ), 7.13 (1H, dd,  $J = 3.5, 5.4$  Hz,  $\text{H}_{\text{py}-5}$ ), 7.22–7.37 (5H, m,  $-\text{C}_6\text{H}_5$ ), 7.60 (1H, dt,  $J = 1.4, 5.4$  Hz,  $\text{H}_{\text{py}-4}$ ), 8.50 (1H, d,  $J = 3.5$  Hz,  $\text{H}_{\text{py}-6}$ ). MS ( $\text{EI}^+$ )  $m/z$  212 ( $\text{M}^+$ ).

(39) The trinuclear copper(II, II, III) complex (**E**) also reacts with 10-methyl-9,10-dihydroacridine ( $\text{AcrH}_2$ ) slowly to give 10-methylacridinium ion ( $\text{AcrH}^+$ ) and the bis(*m*-hydroxo)dicopper(II) complex (**F**) at the low temperature. A very small kinetic deuterium isotope effect (KIE = 1.3) obtained using 9,9-dideuterated derivative ( $\text{AcrD}_2$ ) instead of  $\text{AcrH}_2$  has suggested that oxidation of  $\text{AcrH}_2$  by complex **E** involves an electron-transfer process as the rate-determining step.

(40) Shin, W.; Sundaram, U. M.; Cole, J. L.; Zhang, H. H.; Hedman, B.; Hodgson, K. O.; Solomon, E. I. *J. Am. Chem. Soc.* **1996**, *118*, 3202–3215.

(41) Zoppellaro, G.; Sakurai, T.; Huang, H. *J. Biochem.* **2001**, *129*, 949–953.

(42) Solomon, E. I.; Chen, P.; Metz, M.; Lee, S.-K.; Palmer, A. E. *Angew. Chem., Int. Ed.* **2001**, *40*, 4570–4590.

(43) Perrin, D. D.; Armarego, W. L. F.; Perrin, D. R. *Purification of Laboratory Chemicals*, 4th ed.; Pergamon Press: Elmsford, NY, 1996.

*N*-Benzyl-2-(2-pyridyl)ethylamine (4.24 g, 20 mmol) was treated with ethyl bromide (2.18 g, 20 mmol) and triethylamine (2.02 g, 20 mmol) in refluxing methanol for 2 days. After removal of the solvent by evaporation, the resulting residue was dissolved in  $\text{CH}_2\text{Cl}_2$ , and the solution was washed with 10% aqueous NaOH three times and dried over anhydrous  $\text{K}_2\text{CO}_3$ . After removal of  $\text{K}_2\text{CO}_3$  by filtration, evaporation of the organic solvent gave brown oily material, from which  ${}^{\text{H}}\text{Py}1^{\text{Et,Bz}}$  was isolated by  $\text{SiO}_2$  column chromatographic treatment ( $\text{CHCl}_3$ –AcOEt) in 68% yield.  ${}^1\text{H}$  NMR (300 MHz,  $\text{CDCl}_3$ ):  $\delta$  1.03 (t, 3H,  $J = 7.2$  Hz,  $-\text{CH}_2-\text{CH}_3$ ), 2.58 (q, 2H,  $J = 7.2$  Hz,  $-\text{CH}_2-\text{CH}_3$ ), 2.84–2.99 (m, 4H,  $-\text{CH}_2-\text{CH}_2-\text{Py}$ ), 3.64 (s, 2H,  $-\text{CH}_2-\text{Ph}$ ), 7.08 (1H, dd,  $J = 5.1, 7.2$  Hz,  $\text{H}_{\text{py}-5}$ ), 7.12 (1H, d,  $J = 7.2$  Hz,  $\text{H}_{\text{py}-3}$ ), 7.18–7.29 (5H, m,  $-\text{C}_6\text{H}_5$ ), 7.56 (1H, dt,  $J = 1.8, 7.2$  Hz,  $\text{H}_{\text{py}-4}$ ), 8.50 (1H, dd,  $J = 1.8, 5.1$  Hz,  $\text{H}_{\text{py}-6}$ ). HRMS ( $\text{EI}^+$ )  $m/z$  240.1625 ( $\text{M}^+$ ) calcd for  $\text{C}_{16}\text{H}_{20}\text{N}_2$  240.1626. The  $\alpha,\alpha$ -dideuterated derivative ( ${}^{\text{H}}\text{Py}1^{\text{Et,Bz-d}_2}$ ) was prepared in the same way by using  $\text{PhCD}_2\text{NH}_2$  instead of  $\text{PhCH}_2\text{NH}_2$ , and its purity (>99%) was confirmed by  ${}^1\text{H}$  NMR.

**${}^{\text{Me}}\text{Py}1^{\text{Et,Bz}}$  (*N*-Benzyl-*N*-ethyl-2-(6-methylpyridin-2-yl)ethylamine).** This compound was prepared starting from 6-methyl-2-vinylpyridine and benzylamine through *N*-benzyl-2-(6-methylpyridin-2-yl)ethylamine in a similar manner for the preparation of  ${}^{\text{H}}\text{Py}1^{\text{Et,Bz}}$  in 44% (total yield). Analytical data for *N*-benzyl-2-(6-methyl-2-pyridyl)ethylamine,  ${}^1\text{H}$  NMR (300 MHz,  $\text{CDCl}_3$ ):  $\delta$  2.52 (3H, s,  $-\text{CH}_3$ ), 2.95–3.05 (m, 4H,  $-\text{CH}_2-\text{CH}_2-\text{Py}$ ), 3.82 (s, 2H,  $-\text{CH}_2-\text{Ph}$ ), 6.97 (2H, d,  $J = 7.2$  Hz,  $\text{H}_{\text{py}-3}$  and  $\text{H}_{\text{py}-5}$ ), 7.19–7.35 (5H, m,  $-\text{C}_6\text{H}_5$ ), 7.47 (1H, t,  $J = 7.2$  Hz,  $\text{H}_{\text{py}-4}$ ). MS ( $\text{EI}^+$ )  $m/z$  226 ( $\text{M}^+$ ). Analytical data for  ${}^{\text{Me}}\text{Py}1^{\text{Et,Bz}}$ ,  ${}^1\text{H}$  NMR (300 MHz,  $\text{CDCl}_3$ ):  $\delta$  1.02 (3H, t,  $J = 7.2$  Hz,  $-\text{CH}_2-\text{CH}_3$ ), 2.50 (3H, s,  $-\text{CH}_3$ ), 2.57 (2H, q,  $J = 7.2$  Hz,  $-\text{CH}_2-\text{CH}_3$ ), 2.82–2.96 (4H, m,  $-\text{CH}_2-\text{CH}_2-\text{Py}$ ), 3.63 (2H, s,  $-\text{CH}_2-\text{Ph}$ ), 6.92 (1H, d,  $J = 7.5$  Hz,  $\text{H}_{\text{py}-5}$ ), 6.94 (1H,  $\delta J = 7.5$  Hz,  $\text{H}_{\text{py}-3}$ ), 7.20–7.28 (5H, m,  $-\text{C}_6\text{H}_5$ ), 7.45 (1H, t,  $J = 7.5$  Hz,  $\text{H}_{\text{py}-4}$ ). HRMS ( $\text{EI}^+$ )  $m/z$  254.1786 ( $\text{M}^+$ ) calcd for  $\text{C}_{17}\text{H}_{22}\text{N}_2$ : 254.1783. The  $\alpha,\alpha$ -dideuterated derivative ( ${}^{\text{Me}}\text{Py}1^{\text{Et,Bz-d}_2}$ ) was prepared by using  $\text{PhCD}_2\text{NH}_2$  instead of  $\text{PhCH}_2\text{NH}_2$ , and its purity (>99%) was confirmed by  ${}^1\text{H}$  NMR.

**${}^{\text{H}}\text{Py}1^{\text{Me,Me}}$  (*N,N*-Dimethyl-2-(2pyridyl)ethylamine).** To a solution of 2-(2-aminoethyl)pyridine (3.67 g, 30 mmol), paraformaldehyde (1.81 g, 60 mmol), and acetic acid (3.60 g, 60 mmol) in methanol/water (90/10 mL) was added  $\text{NaBH}_3\text{CN}$  (3.77 g, 60 mmol) slowly, and the resulting mixture was stirred for 5 days. The reaction was then quenched by adding concentrated HCl slowly until the pH of the solution became unity. After removal of the solvent by evaporation, the resulting oily material was dissolved into 1 N aqueous NaOH (100 mL) and was extracted with  $\text{CHCl}_3$  (100 mL x 3). After drying over anhydrous  $\text{K}_2\text{CO}_3$ , evaporation of the organic layer gave brown oily material, from which  ${}^{\text{H}}\text{Py}1^{\text{Me,Me}}$  was isolated by  $\text{SiO}_2$  column chromatography ( $\text{CHCl}_3$ –MeOH) in 80% yield.  ${}^1\text{H}$  NMR (300 MHz,  $\text{CDCl}_3$ ):  $\delta$  2.31 (6H, s,  $-\text{CH}_3$ ), 2.68–2.74 (2H, m,  $-\text{CH}_2-\text{CH}_2-\text{Py}$ ), 2.94–3.00 (2H, m,  $-\text{CH}_2-\text{CH}_2-\text{Py}$ ), 7.11 (1H, ddd,  $J = 0.8, 4.8,$  and  $7.7$  Hz,  $\text{H}_{\text{py}-5}$ ), 7.19 (1H, d,  $J = 7.7$  Hz,  $\text{H}_{\text{py}-3}$ ), 7.59 (1H, dt,  $J = 1.8, 7.7$  Hz,  $\text{H}_{\text{py}-4}$ ), 8.53 (1H, ddd,  $J = 0.8, 1.8,$  and  $4.8$  Hz,  $\text{H}_{\text{py}-6}$ ). HR-MS (EI, pos.) 150.1152 ( $\text{M}^+$ ), calcd for  $\text{C}_9\text{H}_{14}\text{N}_2$ : 150.1157.

**$[\text{Cu}^{\text{I}}(\text{H}^{\text{Et,Bz}}\text{Py}1)(\text{CH}_3\text{CN})]\text{PF}_6$ .** Ligand  ${}^{\text{H}}\text{Py}1^{\text{Et,Bz}}$  (240.4 mg, 1 mmol) was treated with  $[\text{Cu}^{\text{I}}(\text{CH}_3\text{CN})_4]\text{PF}_6$  (372.7 mg, 1 mmol) in THF (7 mL) in a glovebox ( $[\text{O}_2] < 0.1$  ppm,  $[\text{H}_2\text{O}] < 1$  ppm). After stirring the solution for 15 min at room temperature, insoluble material was removed by filtration. Addition of ether (100 mL) to the filtrate gradually gave a pale yellow powder that was precipitated by standing the mixture for several minutes. The supernatant was then removed by decantation, and the remaining pale yellow solid was washed with ether three times and dried to give the copper(I) complex in 87% yield.  ${}^1\text{H}$  NMR (300 MHz, acetone- $d_6$ ):  $\delta$  1.39 (3H, t,  $J = 7.2$  Hz,  $-\text{CH}_2-\text{CH}_3$ ), 2.36 (s, 3H, *coord.*  $\text{CH}_3\text{CN}$ ), 2.93–3.26 (6H, m,  $-\text{CH}_2-\text{CH}_3$  and  $-\text{CH}_2-\text{CH}_2-\text{Py}$ ), 7.33–7.48 (5H, m,  $\text{H}_{\text{py}-3}$ ,  $\text{H}_{\text{py}-5}$ , and  $-\text{C}_6\text{H}_5$ ), 7.56–7.63 (2H, m,  $-\text{C}_6\text{H}_5$ ), 7.93 (1H, dt,  $J = 1.8, 7.2$  Hz), 8.32 (1H, br s,  $\text{H}_{\text{py}-6}$ ). ESI–MS  $m/z$  305.3 ( $[\text{Cu}^{\text{I}}(\text{H}^{\text{Et,Bz}}\text{Py}1)]^+$ ). FTIR (KBr): 840  $\text{cm}^{-1}$  ( $\text{PF}_6^-$ ). Anal. Calcd for  $[\text{Cu}^{\text{I}}(\text{H}^{\text{Et,Bz}}\text{Py}1)(\text{CH}_3\text{CN})]\text{PF}_6$ ,

$\text{C}_{18}\text{H}_{23}\text{N}_3\text{Cu}_1\text{P}_1\text{F}_6$ : C, 44.13; H, 4.73; N, 8.58. Found: C, 44.42; H, 4.57; N, 8.64. Anal. Calcd for  $[\text{Cu}^{\text{I}}(\text{H}^{\text{Et,Bz-d}_2}\text{Py}1)(\text{CH}_3\text{CN})]\text{PF}_6$ ,  $\text{C}_{18}\text{H}_{21}\text{D}_2\text{N}_3\text{Cu}_1\text{P}_1\text{F}_6$ : C, 43.95; H, 5.12; N, 8.54. Found: C, 43.81; H, 4.51; N, 8.35.

**$[\text{Cu}^{\text{I}}(\text{Me}^{\text{Et,Bz}}\text{Py}1)(\text{CH}_3\text{CN})]\text{PF}_6$ .** This compound was prepared in a similar manner for the synthesis of  $[\text{Cu}^{\text{I}}(\text{H}^{\text{Et,Bz}}\text{Py}1)(\text{CH}_3\text{CN})]\text{PF}_6$  by using  ${}^{\text{Me}}\text{Py}1^{\text{Et,Bz}}$  instead of  ${}^{\text{H}}\text{Py}1^{\text{Et,Bz}}$  in 87% yield.  ${}^1\text{H}$  NMR (300 MHz, acetone- $d_6$ ):  $\delta$  1.40 (3H, t,  $-\text{CH}_2-\text{CH}_3$ ), 2.39 (3H, s, *coord.*  $\text{CH}_3\text{CN}$ ), 2.47 (3H, s,  $-\text{CH}_3$ ), 2.95–3.11 (10H, m,  $-\text{CH}_2-\text{CH}_3$ ,  $-\text{CH}_2-\text{CH}_2-\text{Py}$ , and  $-\text{CH}_2-\text{CH}_2-\text{Ph}$ ), 7.23 (1H, d,  $J = 5.7$  Hz,  $\text{H}_{\text{py}-5}$ ), 7.30 (1H, d,  $J = 5.7$  Hz,  $\text{H}_{\text{py}-3}$ ), 7.33–7.42 (3H, m,  $-\text{C}_6\text{H}_5$ ), 7.55–7.60 (2H, m,  $-\text{C}_6\text{H}_5$ ), 7.78 (1H, t,  $J = 5.7$  Hz,  $\text{H}_{\text{py}-4}$ ). FTIR (KBr): 842  $\text{cm}^{-1}$  ( $\text{PF}_6^-$ ). ESI–MS for  $[\text{Cu}^{\text{I}}(\text{Me}^{\text{Et,Bz-d}_2}\text{Py}1)(\text{CH}_3\text{CN})]\text{PF}_6$  (pos.),  $m/z$  319.2 ( $\text{M}^+$ ). Anal. Calcd for  $[\text{Cu}^{\text{I}}(\text{Me}^{\text{Et,Bz}}\text{Py}1)(\text{CH}_3\text{CN})]\text{PF}_6 \cdot \text{H}_2\text{O}$ ,  $\text{C}_{19}\text{H}_{27}\text{N}_3\text{O}_1\text{Cu}_1\text{P}_1\text{F}_6$ : C, 43.72; H, 5.21; N, 8.05. Found: C, 44.21; H, 4.85; N, 7.85.

**$[\text{Cu}^{\text{I}}(\text{H}^{\text{Me,Me}}\text{Py}1)(\text{CF}_3\text{SO}_3)]$ .** To a dry acetone solution (5 mL) of  ${}^{\text{H}}\text{Py}1^{\text{Me,Me}}$  (150 mg, 1 mmol) was added  $[\text{Cu}^{\text{I}}(\text{CH}_3\text{CN})_4]\text{CF}_3\text{SO}_3$  (377 mg, 1 mmol) under anaerobic conditions (Ar). After stirring for 1 h, insoluble material was filtered off. The yellow filtrate was then added dropwise into deaerated ether (200 mL) to give pale yellow powder, which was isolated by decantation and washed with ether three times (67% isolated yield).  ${}^1\text{H}$  NMR (400 MHz, acetone- $d_6$ ):  $\delta$  2.98 (6H, s,  $-\text{CH}_3$ ), 3.39–3.58 (4H, m,  $-\text{CH}_2-\text{CH}_2-\text{Py}$ ), 7.46 (1H, ddd,  $J = 0.8, 4.8,$  and  $7.6$  Hz,  $\text{H}_{\text{py}-5}$ ), 7.59 (1H, d,  $J = 7.6$  Hz,  $\text{H}_{\text{py}-3}$ ), 7.97 (1H, dt,  $J = 1.8, 7.6$  Hz,  $\text{H}_{\text{py}-4}$ ), 8.65 (1H, brs,  $\text{H}_{\text{py}-6}$ ). FTIR (KBr): 638, 1128, 1160, and 1225  $\text{cm}^{-1}$  ( $\text{CF}_3\text{SO}_3^-$ ). ESI–MS (pos.),  $m/z$  213.1 ( $\text{M}^+$ ). Anal. Calcd for  $[\text{Cu}^{\text{I}}(\text{H}^{\text{Me,Me}}\text{Py}1)(\text{CF}_3\text{SO}_3) \cdot 0.5\text{H}_2\text{O}$ ,  $\text{C}_{10}\text{H}_{15}\text{N}_2\text{O}_3.5\text{S}_1\text{F}_3\text{Cu}_1$ : C, 32.3; H, 4.07; N, 7.53. Found: C, 32.6; H, 3.86; N, 7.63.

**$[\text{Cu}^{\text{I}}(\text{H}^{\text{Et,Bz-d}_2}\text{Py}1)(\text{PPh}_3)]\text{PF}_6$ .** To a suspension of  $[\text{Cu}^{\text{I}}(\text{H}^{\text{Et,Bz-d}_2}\text{Py}1)(\text{CH}_3\text{CN})]\text{PF}_6$  (49.1 mg, 0.1 mmol) in THF (2 mL) was added a THF (3 mL) solution of triphenylphosphine (52.5 mg, 0.2 mmol) in a glovebox ( $[\text{O}_2] < 0.1$  ppm). After stirring the mixture for 5 min at room temperature, an insoluble material was filtered off. The colorless filtrate was then added dropwise into ether (70 mL) to give white powder, which was isolated by decantation and washed with ether three times (83% isolated yield). Single crystals (colorless prism) for X-ray structure determination were obtained by recrystallization from methanol/ether.  ${}^1\text{H}$  NMR (400 MHz, acetone- $d_6$ ):  $\delta$  2.59 (6H, s,  $-\text{CH}_3$ ), 2.89–2.96 (2H, m,  $-\text{CH}_2-\text{CH}_2-\text{Py}$ ), 3.22–3.29 (2H, m,  $-\text{CH}_2-\text{CH}_2-\text{Py}$ ), 7.41 (1H, ddd,  $J = 0.8, 5.2,$  and  $7.6$  Hz,  $\text{H}_{\text{py}-5}$ ), 7.50–7.62 (16H, m,  $\text{H}_{\text{py}-3}$  and aromatic), 8.00 (1H, dt,  $J = 1.6, 7.6$  Hz,  $\text{H}_{\text{py}-4}$ ), 8.42 (1H, ddd,  $J = 0.8, 1.6,$  and  $5.2$  Hz,  $\text{H}_{\text{py}-6}$ ). FTIR (KBr): 840  $\text{cm}^{-1}$  ( $\text{PF}_6^-$ ). ESI–MS (pos.),  $m/z$  566.9 ( $\text{M}^+$ ). Anal. Calcd for  $[\text{Cu}^{\text{I}}(\text{H}^{\text{Et,Bz-d}_2}\text{Py}1)(\text{PPh}_3)]\text{PF}_6$ ,  $\text{C}_{34}\text{H}_{33}\text{D}_2\text{N}_2\text{P}_3\text{F}_6\text{Cu}$ : C, 57.26; H, 5.23; N, 3.93. Found: C, 57.52; H, 5.24; N, 3.72.

**$[\text{Cu}^{\text{I}}(\text{H}^{\text{Me,Me}}\text{Py}1)(\text{PPh}_3)]\text{PF}_6$ .** To a suspension of  $[\text{Cu}^{\text{I}}(\text{CH}_3\text{CN})_4]\text{PF}_6$  (186 mg, 0.5 mmol) in  $\text{CH}_2\text{Cl}_2$  (2 mL) was added a  $\text{CH}_2\text{Cl}_2$  (3 mL) solution of  ${}^{\text{H}}\text{Py}1^{\text{Me,Me}}$  (75.0 mg, 0.5 mmol) under anaerobic conditions (Ar in a glovebox). After stirring the mixture for 30 min, triphenylphosphine (131 mg, 0.5 mmol) was added into the resulting solution. After additional stirring for 30 min, an insoluble material was filtered off. The colorless filtrate was then added dropwise into deaerated ether (100 mL) to give white powder, which was isolated by decantation and washed with ether three times (64% isolated yield). Single crystals (colorless prism) for X-ray structure determination were obtained by recrystallization from  $\text{CH}_2\text{Cl}_2$ /ether.  ${}^1\text{H}$  NMR (400 MHz, acetone- $d_6$ ):  $\delta$  2.59 (6H, s,  $-\text{CH}_3$ ), 2.89–2.96 (2H, m,  $-\text{CH}_2-\text{CH}_2-\text{Py}$ ), 3.22–3.29 (2H, m,  $-\text{CH}_2-\text{CH}_2-\text{Py}$ ), 7.41 (1H, ddd,  $J = 0.8, 5.2,$  and  $7.6$  Hz,  $\text{H}_{\text{py}-5}$ ), 7.50–7.62 (16H, m,  $\text{H}_{\text{py}-3}$  and aromatic), 8.00 (1H, dt,  $J = 1.6, 7.6$  Hz,  $\text{H}_{\text{py}-4}$ ), 8.42 (1H, ddd,  $J = 0.8, 1.6,$  and  $5.2$  Hz,  $\text{H}_{\text{py}-6}$ ). FTIR (KBr): 839  $\text{cm}^{-1}$  ( $\text{PF}_6^-$ ). ESI–MS (pos.),  $m/z$  474.9 ( $\text{M}^+$ ). Anal. Calcd for  $[\text{Cu}^{\text{I}}(\text{H}^{\text{Me,Me}}\text{Py}1)(\text{PPh}_3)]\text{PF}_6$ ,  $\text{C}_{27}\text{H}_{29}\text{N}_2\text{P}_3\text{F}_6\text{Cu}$ : C, 52.2; H, 4.71; N, 4.51. Found: C, 52.3; H, 4.69; N, 4.51.

**$[\text{Cu}^{\text{II}}(\text{H}^{\text{Me,Me}}\text{Py}1)(\mu\text{-OH})_2](\text{CF}_3\text{SO}_3)_2$ .** The reaction of  $[\text{Cu}^{\text{II}}\text{Cu}^{\text{III}}(\text{H}^{\text{Me,Me}}\text{Py}1)_3(\mu_3\text{-O})_2](\text{CF}_3\text{SO}_3)_3$  (1.7 mM) and DBP (10 mM) was carried out in acetone at  $-80$  °C for 24 h. Evaporation of the solvent gave a

blue color residue, which was washed with ether (30 mL  $\times$  2), collected by filtration, and dried under vacuo. Single crystals (blue prism) for X-ray structure determination were obtained by recrystallization from acetone/ether. FTIR (KBr): 3570  $\text{cm}^{-1}$  ( $\mu\text{-OH}$ ), 636, 1028, 1159, and 1225  $\text{cm}^{-1}$  ( $\text{CF}_3\text{SO}_3^-$ ). ESI-MS (pos.),  $m/z$  608.8 ( $\text{M}^+$ ). Anal. Calcd for  $[\text{Cu}^{\text{II}}(\text{H}^{\text{Me,Me}}\text{Py})_2(\mu\text{-OH})_2](\text{CF}_3\text{SO}_3)_2$ ,  $\text{C}_{20}\text{H}_{30}\text{N}_4\text{O}_8\text{S}_2\text{F}_6\text{Cu}_1$ : C, 31.78; H, 3.98; N, 7.38. Found: C, 31.78; H, 3.97; N, 7.40.

**Product Analysis. Oxidative N-Dealkylation Reaction.** The copper(I) complex (0.15 mmol) was dissolved into deaerated acetone (10 mL), and the solution was cooled to  $-78^\circ\text{C}$  using an acetone/dry ice bath, and then dry  $\text{O}_2$  gas was introduced into the solution at this temperature. The resulting solution was stirred for several hours at  $-78^\circ\text{C}$ . After evaporation of the solvent, the oxidized product was dissolved into 2.8 M aqueous  $\text{NH}_3$  (25 mL), extracted with  $\text{CH}_2\text{Cl}_2$  (25 mL  $\times$  3), and dried over  $\text{K}_2\text{CO}_3$ . Identification and quantification of the oxidized products were carried out by  $^1\text{H}$  NMR and mass spectroscopy. Yields of the oxidation products, benzaldehyde and *N*-ethyl-2-(2-pyridyl)-ethylamine, were 25–35% based on the  $\text{Cu}_2\text{O}_2$  complex (theoretical maximum is 50%). The lower yields of the oxidation products are due to difficulty in recovering the small amounts of volatile benzaldehyde and the amine product which is highly soluble in water.

**Oxygenation of 2,4-Di-*tert*-butylphenol (DBP).** The bis( $\mu_3$ -oxo) trinuclear copper(II, II, III) complex was generated by the reaction of  $[\text{Cu}^{\text{I}}(\text{H}^{\text{Me,Me}}\text{Py})_2(\text{CF}_3\text{SO}_3)]$  (0.10 mmol) and  $\text{O}_2$  gas at  $-80^\circ\text{C}$  in anhydrous acetone (20 mL) for 10 min. After removal of excess  $\text{O}_2$  by bubbling Ar gas into the solution for 10 min, a solution of DBP (0.2 mmol) in 0.5 mL of anhydrous acetone was added into the solution, and the mixture was stirred for 24 h at this temperature. After evaporation of the solvent, 50 mL of ether was added to the remaining residue, and the insoluble material was removed by filtration. The separated solid was further washed with additional ether (30 mL  $\times$  3), and the combined ether solution was concentrated to give an organic material, from which 3,5,3',5'-tetra-*tert*-butyl-biphenyl-2,2'-diol was obtained in 97% yield.

**Manometry.** Typically, the  $\text{O}_2$ -uptake measurement was carried out on the reaction of  $[\text{Cu}^{\text{I}}(\text{H}^{\text{Et,Bz-d}_2}\text{Py})_2(\text{CH}_3\text{CN})]\text{PF}_6$  (158.5 mg, 0.304 mmol) in deaerated acetone (3 mL) at  $-80^\circ\text{C}$ . The volume of  $\text{O}_2$  consumed during the oxygenation reaction of the copper(I) complex was determined to be 3.90 mL as a difference of the  $\text{O}_2$  consumption between  $\text{Cu}/\text{O}_2$  intermediate formation and the blank solution without the reactants under exactly the same conditions using a manometer designed for the small-scale reaction. Thus, the stoichiometry of  $\text{Cu}:\text{O}_2$  was calculated to be 2:1 ( $\pm 0.05$ ) for the formation of  $[\{\text{Cu}^{\text{II}}(\text{H}^{\text{Et,Bz-d}_2}\text{Py})_2(\mu\text{-O}_2)\}(\text{PF}_6)_2]$ . The stoichiometry of  $\text{Cu}:\text{O}_2$  for the formation of  $[\{\text{Cu}^{\text{III}}(\text{H}^{\text{Et,Bz-d}_2}\text{Py})_2(\mu\text{-O})_2\}(\text{PF}_6)_2]$  and  $[\{\text{Cu}^{\text{II}}\text{Cu}^{\text{III}}(\text{H}^{\text{Me,Me}}\text{Py})_3(\mu_3\text{-O})_2\}(\text{CF}_3\text{SO}_3)_3]$  was determined as 2:1 ( $\pm 0.05$ ) and 3:1 ( $\pm 0.05$ ), respectively, by the same procedure.

**Kinetics.** The copper-dioxygen complexes were generated in situ by the reaction of Cu(I) complex and dry  $\text{O}_2$  gas (introduced by gentle bubbling for a few minutes) in a UV-vis cell (1 cm or 1 mm path length) which was held in a Unisoku thermostated cell holder designed for the low-temperature experiments (fixed within  $\pm 0.5^\circ\text{C}$ ). Rate constants for the formation and decay of the copper-dioxygen complexes were determined by monitoring an increase and decrease in the absorption bands due to the intermediate complexes.

Oxidation of 2,4-di-*tert*-butylphenol (DBP) by the bis( $\mu_3$ -oxo) trinuclear copper(II, II, III) complex was started by adding the substrate with use of a microsyringe into the solution at  $-90^\circ\text{C}$  (first process) and  $-70^\circ\text{C}$  (second process), after excess  $\text{O}_2$  was removed by bubbling Ar gas into the solution of the bis( $\mu_3$ -oxo) trinuclear copper complex for 5 min. The reaction was followed by monitoring a decrease in absorbance at 515 nm due to the bis( $\mu_3$ -oxo) trinuclear copper(II, II, III) complex.

**Resonance Raman Measurements.** The 363.8 nm line of an  $\text{Ar}^+$  ion laser (model 2080 Spectra Physics) was used as the exciting source of the Raman scattering. Resonance Raman spectra were detected with a liquid nitrogen cooled CCD detector (Model LN/CCD-1100  $\times$  330PB, Princeton Instruments) attached to a 1 m single polychromator (Model MC-100DG, Ritsu Oyo Kogaku). The mechanical slit width and slit height of the polychromator were set to 200 and 20 mm, respectively. The corresponding spectral slit width was 11.8  $\text{cm}^{-1}$ , and a wavenumber width per one channel of the array detection was 1.1  $\text{cm}^{-1}$ . The laser power used was 2.5 mW at the sample point. All measurements were carried out at  $-100 (\pm 2)^\circ\text{C}$  with a spinning cell (1000 rpm). Raman shifts were calibrated with indene, and accuracy of the peak positions of the Raman bands was  $\pm 1 \text{ cm}^{-1}$ .

**X-ray Structure Determination.** The single crystals were mounted on a glass capillary or a CryoLoop (Hampton Research Co. Ltd.). Data of X-ray diffraction were collected by a Rigaku RAXIS-RAPID imaging plate two-dimensional area detector using graphite-monochromated  $\text{Mo K}\alpha$  radiation ( $\lambda = 0.71070 \text{ \AA}$ ) to  $2\theta$  max of  $55^\circ$ . All of the crystallographic calculations were performed using Crystal Structure software package of the Molecular Structure Corp. [Crystal Structure: Crystal Structure Analysis Package version 2.0, Molecular Structure Corp. and Rigaku Corp. (2001)]. The crystal structure was solved by the direct methods and refined by the full-matrix least squares using SIR-92. All non-hydrogen atoms and hydrogen atoms were refined anisotropically and isotropically, respectively. Atomic coordinates, thermal parameters, and intramolecular bond distances and angles are deposited in the Supporting Information (CIF file format).

**Acknowledgment.** This work was financially supported in part by Grants-in-Aid for Scientific Research on Priority Area (No. 11228206) and Grants-in-Aid for Scientific Research (No. 13480189) from the Ministry of Education, Culture, Sports, Science, and Technology, Japan.

**Supporting Information Available:** The resonance Raman spectra of the oxygenated intermediate derived from  $[\text{Cu}^{\text{I}}(\text{H}^{\text{Me,Me}}\text{Py})_2(\text{CF}_3\text{SO}_3)]$  at the lower concentration (0.2 mM) in acetone (Figure S1), the UV-vis spectral change for the oxygenation reaction of  $[\text{Cu}^{\text{I}}(\text{H}^{\text{Et,Bz-d}_2}\text{Py})_2(\text{CH}_3\text{CN})]\text{PF}_6$  ( $3.0 \times 10^{-3} \text{ M}$ ) at  $-94^\circ\text{C}$  in acetone (Figure S2), and the kinetic data for the reaction between **E** and DBP in acetone at  $-70^\circ\text{C}$  (Figure S3) (PDF). X-ray structural determination and details of the crystallographic data are supplied as a CIF file. This material is available free of charge via the Internet at <http://pubs.acs.org>.

JA026047X